

## Final Technical Report

# The Development of Open Water-lubricated Polycrystalline Diamond (PCD) Thrust Bearings for Use in Marine Hydrokinetic (MHK) Energy Machines

### DOE Award Number:

DE-EE0003633

### Project Period:

09/01/2010 to 08/30/2012

### Principle Investigators and Authors:

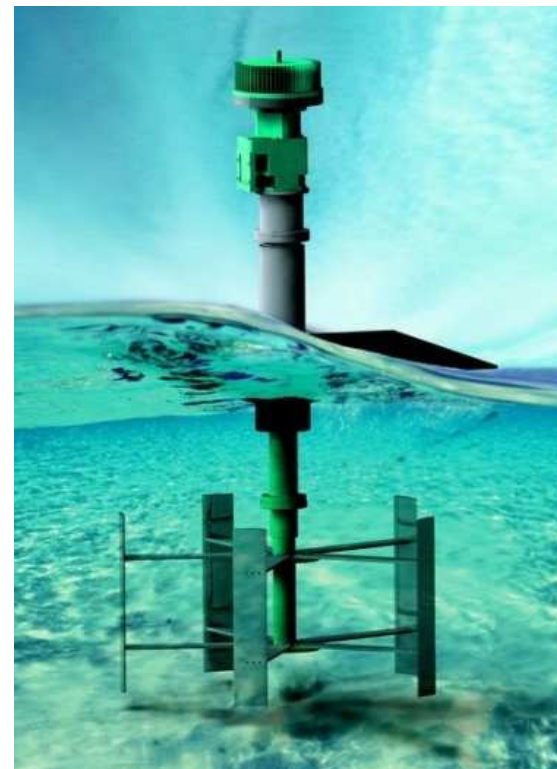
Craig H. Cooley, P.E.  
801 319 0891  
[ccoley@ussynthetic.com](mailto:ccoley@ussynthetic.com)

Professor Michael M. Khonsari, Ph.D.  
225 578 9192  
[khonsari@me.lsu.edu](mailto:khonsari@me.lsu.edu)

Brent Lingwall  
801 228 7986  
[blingwall@ussynthetic.com](mailto:blingwall@ussynthetic.com)

### Date of report:

November 31, 2012



THIS PAGE INTENTIONALLY LEFT BLANK

Acknowledgments:

The authors would like to thank the United States' Department of Energy (DOE) for providing a grant to fund this research. This report is based upon work supported by the U. S. Department of Energy under Award No. DE EE0003633. The authors would also like to thank US Synthetic Corporation for permission to author and to submit this report and other papers based on this work. Finally, thanks to Brigham Kindell, Kevin Fernelius, Cody Knuteson, Justin Rhodes, Troy Campbell, and all US Synthetic Bearings employees for manufacturing bearing test samples and carrying out the laboratory tests.

Disclaimer:

Any findings, opinions, and conclusions or recommendations expressed in this report are those of the authors and do not necessarily reflect the views of the Department of Energy.

THIS PAGE INTENTIONALLY LEFT BLANK

## Table of Contents

- i. Cover page
- ii. Acknowledgement and disclaimer
- iii. Table of contents
- iv. List of acronyms
- v. List of figures
- vi. List of tables and appendices
- vii. Executive summary

- 1. Introduction
- 2. Background
  - 2.1. Polycrystalline diamond (PCD)
  - 2.2. Bearing design considerations I
    - 2.2.1. Incline-pad and pivoted thrust bearing design
    - 2.2.2. PCD thrust bearings and highly-loaded bearing operation
    - 2.2.3. Diamond-pad shapes
    - 2.2.4. Summary design considerations I
- 3. Bearing development and experimental methodology
  - 3.1. Analytical model development
- 4. Experimental procedure, results and discussion
  - 4.1. Experimental procedure
  - 4.2. Types of tests performed and their purpose
  - 4.3. Results and discussion
    - 4.3.1. First set of experiments
      - 4.3.1.1. Friction tests
      - 4.3.1.2. Constant load life tests
      - 4.3.1.3. Lessons learned from first set of experiments
      - 4.3.1.4. Design recommendations based on the first set of experiments
    - 4.3.2. Second and third set of experiments
      - 4.3.2.1. Friction tests
      - 4.3.2.2. Constant load life tests
      - 4.3.2.3. Bearing load capacity tests
      - 4.3.2.4. Lessons learned from the second and third set of experiments
      - 4.3.2.5. Design recommendations based on the second and third set of experiments
    - 4.3.3. Cyclical loading experiments
      - 4.3.3.1. Life (wear) observations
      - 4.3.3.2. Conclusions from the cyclical loading experiments
- 5. Design considerations II

- 5.1. Simplified design charts for round shaped pads
- 5.2. Lift off calculations and Stribeck behavior
- 6. Field application of proto-type diamond bearings
- 7. Study summary and conclusions
- 8. Accomplishments
- 9. Recommendations
- 10. References and bibliography
- 11. Appendices
  - 11.1. Final progress report organized in the SOPO format
  - 11.2. Discussion of TRL 4 justification
  - 11.3. Example analysis of a round pad bearing

List of acronyms

Acronym	Definition
ARPA-E	Advanced Research Projects Agency - Energy
C	Circular shaped bearing pads
COF	Coefficient of Friction
DOE	Department of Energy
GPM	Gallons per Minute
MHK	Marine Hydrokinetic
PCD	Polycrystalline Diamond
PDC	Polycrystalline Diamond Compact (Cutting element on petroleum drill bits)
R	Bearing rotating ring, rotor
Ra	Surface roughness, $\mu$ inches
S	Bearing stationary ring' stator
SOPO	Schedule of Project Objectives
TP	Transition Point
TRL	Technology Readiness Level
USPTO	United States Patent and Trademark Office
USS	US Synthetic Corporation
W	Wedge shaped bearing pads
WC	Tungsten Carbide

THIS PAGE INTENTIONALLY LEFT BLANK

List of figures:

Figure	Description	page
2-1	Picture of Tracy Hall	3
2-2	Carbon phase diagram	4
2-3	High temperature high pressure press	5
2-4	Synthetic diamond crystals	5
2-5	PCD material micrograph	6
2-6	Diamond powder, cube assembly and finished PDC	6
2-7	Drill bit for drilling oil and gas wells	8
2-8	Thrust and radial PCD bearings for oil and gas down hole tools	8
2-9	PCD compact brazed into a bearing ring	8
2-10	Taper bearing schematic (inclined pad with parallel extension), tilting pad schematic, and flat parallel surface schematic (source: Khonsari & Booser, 2008)	10
2-11	Film thickness variation with change in pivot location	11
2-12	Stribeck curve with labeled lubrication regimes plotted as a function of viscosity, rotational speed, and pressure	12
3-1	Tilting pad thrust bearing with continuous runner	13
3-2	Hypothetical turbine with diamond bearings	14
4-1	Thrust bearing test stand	15
4-2	Thrust bearing test apparatus schematic	15
4-3	Bearing configurations tested during this study	17
4-4	Engaged surface area plot for bearing configuration	18
4-5	Flow area plot for bearing configuration	18
4-6	PCD bearing thermal failures	20
4-7	Round and wedge shaped PCD pad performance in oil	21
4-8	COF versus rotational speed during friction testing for 11CR/12CS, 16WR/15WS and 15WR/16WS	22
4-9	COF versus time for 11CR/12CS demonstrating extended 'wear-in' behavior	24
4-10	COF versus time during constant load life testing of 11CR/12CS, 16WR/15WS and 15WR/16WS	25
4-11	COF versus RPM during friction testing for all configurations	27
4-12	Repeat COF versus RPM during 6000 lbf friction testing for 11CR/12CS, 15WR/16WS, 12WR/15WS, and 15WR/15WS	28
4-13	COF versus time during constant load life testing for all configurations	29
4-14	Axial load at failure	31
4-15	Specific load at failure	31
4-16	Load at failure for 400 RPM failure tests	32
4-17	Load at failure for 1000 RPM failure tests	32
4-18	Torque versus load during 1000 RPM failure tests	34

4-19	Temperature difference versus load during 1000 RPM failure tests	34
4-20	Specific load at failure versus flow rate	36
4-21	Torque over 6000 cycles in the 12WR/15WS and 15WR/16WS life tests	38
4-22	Surface roughness over 6000 cycles in the 12WR/15WS life test	39
4-23	Average wear rate during the 6000 cycle life test	39
5-1	Dimensionless hydrodynamic load plotted as a function of film thickness ratio	42
5-2	Variation of hydrodynamic COF for a circular, corresponding modified, and square pads	42
5-3	Friction behavior as a function of speed	44
6-1	Diamond radial bearings model rendition of bearings supplied to the University of Alaska for simulated field evaluation	45

## List of Tables

Table	Description	page
1	Properties of PCD and other hard materials for comparison	7
2	‘Wear-in’ time and bearing engagement area	30

## List of Appendices

Appendix	Description	page
11.1	Final progress report organized in SOPO format	57
11.2	Discussion of TRL 4 justification	65
11.3	Example analysis of round pad bearing	69

THIS PAGE INTENTIONALLY LEFT BLANK

## Executive Summary

- The marine hydrokinetic (MHK) environment is harsh and conventional bearing technology is not adequate.
- For MHK to be economical the bearings must be efficient and have long life.
- PCD diamond bearings have worked well in oil and gas down-hole tool applications for years.
- This work investigated the use of PCD bearings for use in MHK machines.
- Existing US Synthetic (USS) lab equipment was modified to simulate the MHK loading and environmental conditions.
- Three generations of diamond bearings were designed and evaluated for use in MHK machines. Each subsequent generation was modified for better performance in the anticipated MHK environment. The final resulting designs were life tested.
- Life and performance testing showed that PCD diamond bearings have sufficient life and load carrying ability to function well in the MHK environment.
  - These bearings work well when they are in rubbing contact, and when they are hydrodynamic (there is a lubricating film between the surfaces).
  - The pre-dominate mode of operation (rubbing or fluid film) will dictate the design of the bearing.
  - Though the ‘wear-in’ of the bearings was minimal, the design of the bearing mounts should accommodate slight ‘wear in’ of the bearings.
- Some preliminary analysis aimed at providing design tools for diamond bearings was conducted using the experimental data obtained during this work. It was found that a complete model was beyond the proposed scope. Highlights of accomplishments are as follows:
  - Developed a design method for round bearing pads and conducted an analysis to predict lift off (the beginning of hydro-dynamic bearing behavior) for wedge-shaped pads.
  - A foundation of understanding has been laid for further analytical modeling work.
- US Synthetic participated in 2011 and 2012 ARPA-E and 2011 Clean Tech symposiums by exhibiting at the show case event in the former and presenting in the later.
- Test bearings were provided to the University of Alaska for further testing and evaluation prior to use in a commercial MHK setting.
- One patent and two published papers have directly resulted from this work.
- This work moved diamond bearings from TRL 3 to TRL 4; thus they can now be applied in prototype MHK machines.
- US Synthetic has reached out to builders of MHK machines and there are at least three potential customers interested in evaluating these bearings.

THIS PAGE INTENTIONALLY LEFT BLANK

## 1. Introduction

A polycrystalline diamond (PCD) bearing has been developed that will operate successfully in Marine Hydro-kinetic (MHK) machine applications. PCD bearings represent a new class of bearings that have, heretofore, not been extensively studied. This work makes significant contributions to understanding the performance of these bearings.

The study results will be presented in the main body of the report approximately as outlined in the Schedule of Project Objectives (SOPO). This organization will, hopefully, help in understanding the thought and reasoning process as progress toward the final MHK diamond bearing designs was made. (Appendix 11.1 is an abridged summary of the work performed during the project and it is formatted like the quarterly reports.)

The environment for MHK machines is difficult and presents challenges to conventional bearing technology. Conventional roller and sliding bearings require protection from the submerged environment and must be provided with lubrication. In addition they are subjected to frequent starting and stopping, contaminants and long time periods between maintenance. These are challenges that are beyond conventional marine bearing technology. The goal of this work was to provide to the MHK community a robust and simple bearing technology that would contribute to the commercial success of MHK by meeting the challenges of the MHK applications.

This work proposes PCD for bearings in the MHK application. PCD is not in the lexicon of materials used daily by most engineers. It is considered exotic, but it should not be. Recent work by US Synthetic (USS) has shown that its range of economic application can and should be greatly expanded. Among the properties that make PCD an excellent bearing material are: thermal conductivity approximately twelve times that of steel, hardness that surpasses any other known material, exceptional strength and resistance to abrasion.

PCD has found use as bearings in the oil and gas drilling environment where it has been used in down-hole drilling tools such as drilling motors, turbines, and steering devices. In this environment PCD has proven to be economical and operate successfully even while being subjected to abrasive lubrication, shock loading, and extended life requirements. It is believed that these attributes that make PCD bearings successful in application involving the oil and gas well bore will also contribute to making it successful in MHK applications.

One key similarity is the cost of bearing replacement in both applications. Replacing drilling equipment requires the drilling rig to stop drilling and extract and replace a long string of drill pipe (referred to as 'tripping') which is expensive (off shore it costs over \$500,000 per trip) and

drives the economics that makes cost effective the use of a more expense material like diamond (PCD) for use in bearings. The same would be true of an MHK application which might require the use of special ships or rigs to extract the machine and replace failed equipment. It is easy to imagine that maintenance of MHK machines would be equivalent to, or even more expensive than, the trip necessary to change down-hole drilling tools.

PCD bearings applied in MHK would make the use of the surrounding water as a lubricant possible. This in turn would allow for simple and robust bearing designs, which minimize maintenance and eliminate the potential of environmental lubricant leaks. Further the hardness and abrasive resistance of PCD would also minimize effects of sediment contamination on bearing life and performance, a potential issue in near shore tidal applications. In addition sediment contamination is less likely to affect bearing performance when PCD bearings are used. Finally, USS has demonstrated that these bearings operate effectively regardless of speed. Slow operation where the bearing surfaces are rubbing can be accommodated as can faster operation where a fluid-film is present (this will be clarified later). The ability to do this makes the start/stop operation of tidal MHK machines a non-problem.

An additional goal of this work was to move the technology readiness level (TRL) of PCD bearing technology forward, specifically from TRL 3 to TRL 4. To accomplish this a project objective and a specific set of tasks were identified and documented in a ‘Statement of Project Objectives’ (SOPO) document that included seven specific tasks to be accomplished. The project objective as stated in the SOPO is: “to demonstrate that a diamond thrust bearing will have the necessary life and operate with the necessary efficiency (lack of friction) under conditions similar to those expected in MHK applications.” To that end the tasks enumerated in the SOPO were completed and the results and conclusions for each task enumerated in the SOPO are reported in this document. The specific results for each task are given in Appendix 11.1.

The work presented shows that PCD bearings submerged in a water environment easily survive the anticipated MHK static and cyclical loads. In addition a simulation of start/stop operations demonstrated an anticipated life that could be equal to at least 11.5 years. In addition a basic understanding of the important performance variables was won, making it possible to make approximate design recommendations based on the bearings primary mode of operation, be it primarily slow running with bearing surfaces rubbing or quicker operation with bearing surfaces separated by a fluid-film.

Finally, USS has made a successful outreach to industry and the R&D community at large. Two papers have been accepted and will be presented over the course of the next year. A patent has been applied for and US Synthetic Bearings has identified at least three potential customers who seem willing to evaluate and perhaps test PCD diamond technology in their prototype MHK machines.

## 2.0 Background

### 2.1 Polycrystalline diamond (PCD)

The invention of man-made diamond is generally attributed to Tracy Hall (Figure 2-1) who was a high pressure high temperature material researcher at General Electric, Schenectady, NY circa 1954 (Hazen, 1999). Working with high pressure and temperature equipment, he and a team of researchers were the first to transform graphite to diamond crystals (Figure 2-2).



**Figure 2-1.** Dr. Tracy Hall, researcher at General Electric and key contributor to the invention of the man-made diamond. (source: <http://www.novatek.com>)

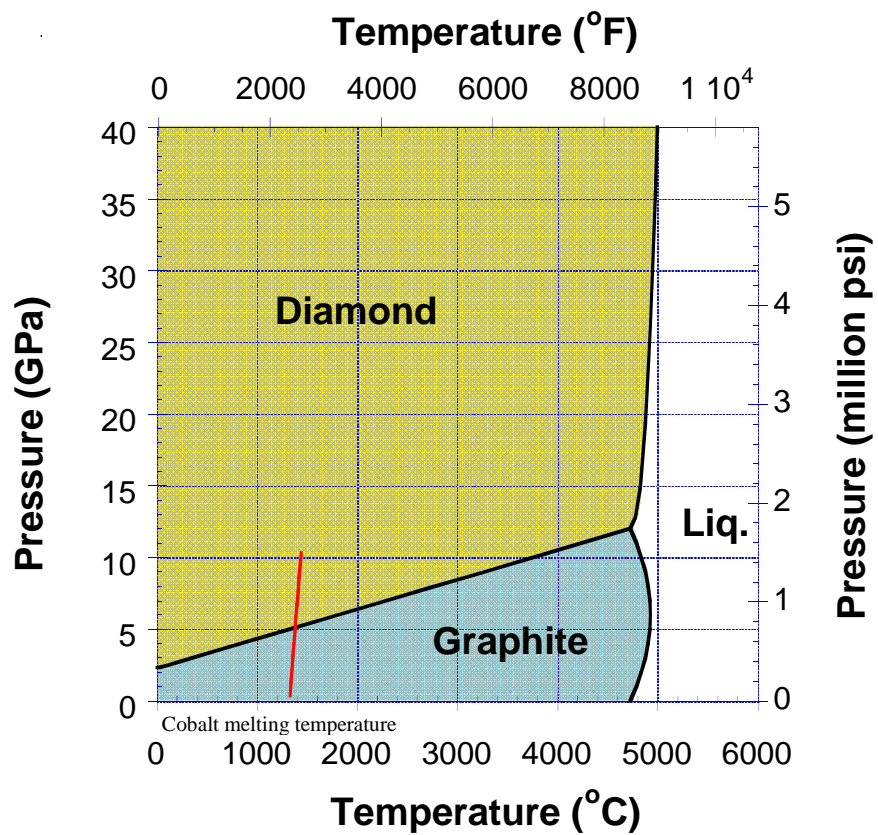


**Figure 2-2.** Carbon phase diagram: graphite with added heat and pressure form diamond. (source: US Synthetic internal presentation)

Now routinely, man-made or synthetic diamond is grown at high pressure (1,000,000 psi) and high temperature (2700 degrees F) using large high pressure high temperature presses like that shown in Figure 2-3 that mimic the conditions that produce natural diamond in the earth. The product of this process are individual synthetic diamond crystals like those shown in Figure 2-4.

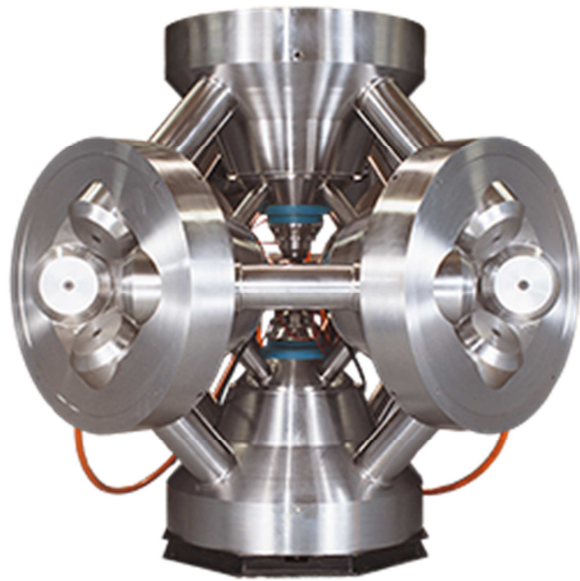


**Figure 2-3.** A high pressure high temperature press used to produce synthetic diamond. (source: USS internal presentation)



**Figure 2-4.** Diamond powder (left) and individual synthetic diamond crystals (right). (source: USS internal presentation)

These single synthetic diamond crystals can be then sintered together to form polycrystalline diamond or PCD. Like the synthesis process for single diamond crystals the sintering of individual diamond grains into polycrystalline diamond takes place under the same high pressure and temperature environment (Figure 2-5).

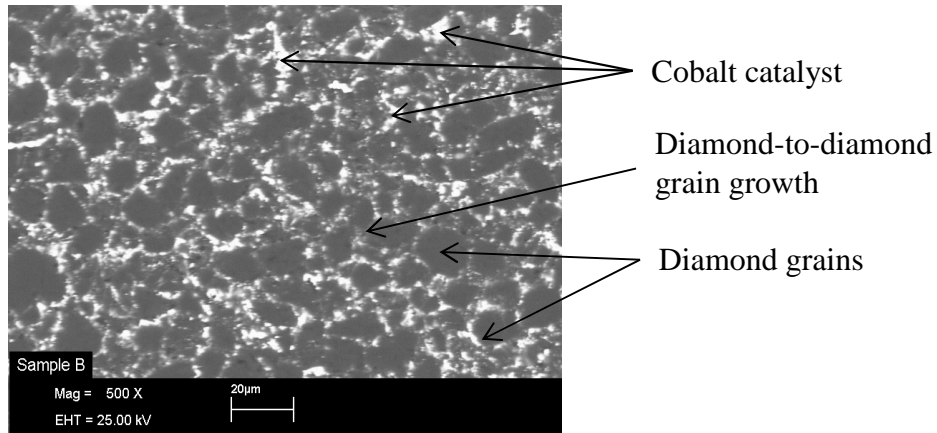


**Figure 2-5.** Scanning electron microscope (SEM) micrograph of PCD at 500X magnification.

The USS process places diamond grit on a tungsten carbide, WC, substrate. This assembly is then placed in a proprietary cube which contains an internal furnace which, in turn, is placed in the high pressure press as shown in Figure 2-6. Cobalt that is in the WC migrates through the diamond and facilitates diamond to diamond bonding and diffusion bonding to the WC substrate. The end product is a right circular cylinder with a diamond layer between 1 and 4 mm thick. The diamond table thickness differentiates PCD from other diamond like coatings that often are .025" thick or less (Surface Technology, 2012). The substantial thickness proves to be an advantage for heat conduction and strength. A disadvantage is that this material must be made in a limited volume high temperature high pressure press which in turn limits the size of each PCD part. Larger surfaces must be put together in mosaic fashion.

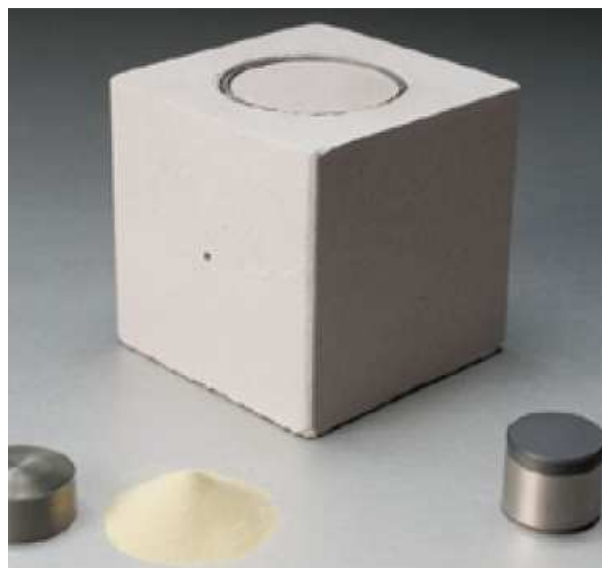


**Figure 2-6.** Diamond powder, tungsten carbide substrate (WC), high pressure/high temperature cube, and a complete diamond compact.

PCD has the advantage that there are no single planes of preferred fracture like those found in single diamond crystals. This is because of the random orientation of all the single crystals that make up the structure of PCD. In addition, PCD has outstanding thermal and strength properties which are enumerated in Table 1. These properties make PCD an excellent choice for a bearing material.

**Table 1.** Properties of PCD and other hard materials for comparison.

Properties	Polycrystalline Diamond (PCD)	Tungsten Carbide	Steel (4140)	Silicon Nitride	Silicon Carbide
Coefficient of Friction	0.05-0.08**	0.2-0.25†	0.42‡	--	--
Thermal Conductivity (W/m*K)	543	70	42.6	30	85
Fracture Toughness (MPa <sup>1/2</sup> m)	13-15	10-25	50	4	3.5-4
Hardness (GPa, Knoop)	49.8	1.8	0.2	1.8	2.4
Compressive Strength (GPa)	6.9-7.6	2.68	--	--	2.5
Young's Modulus (GPa)	841	669-696	205	296	434
Tensile Strength (MPa)	1,300-1,600	334	415	520	500

\*AS1 4140 Steel, annealed at 815°C (1500°F) furnace cooled 11°C (20°F)/hour to 665°C (1230°F), air cooled, 25 mm (1 in.) round(1100°F) temper

\*\* PCD on PCD in H<sub>2</sub>O, dynamic, dynamic

†Tungsten Carbide on Tungsten Carbide, static

‡Steel (Hard) on Steel (Hard), dynamic

YAt 100°C

Sources: Bertagnolli, US Synthetic; Roberts et al., De Beers; Cooley, US Synthetic; Jiang Qian, US Synthetic; Glowka, SNL; Sexton, US Synthetic; Lin, UC Berkeley, MatWeb.com, Cerco

PCD product has been used for years in machining and grinding applications. One well proven use is as cutting elements in drill bits used for drilling oil and gas wells (Figure 2-7). PCD has found application as bearing pads for a number of oil and gas related applications (Figure 2-8). For example, bearings use PCD pads cemented on the WC substrate and brazed into a ring, see Figure 2-9. Unlike conventional bearings which have one half the bearing configured with discrete pads and the other half with a runner which has a continuous bearing surface, diamond bearings have both the stator and rotator configured with discrete pads. This is a consequence of the limit on part size as described previously.



**Figure 2-7.** Diamond is used in drill bits and drilling tools and applied in the drilling of oil and gas wells. Shown are a steering assembly and a PDC drag bit.



**Figure 2-8.** Diamond is used in bearings for the oil and gas industry.

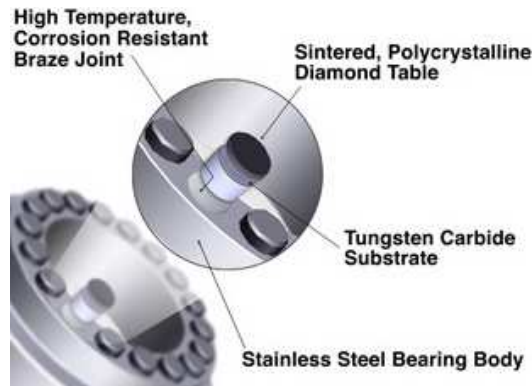


**Figure 2-9.** PCD compacts are brazed into a metal ring to fabricate a bearing.

## 2.2. Bearing design considerations I

In conventional slider bearings, the surfaces are completely separated with a “relatively thick” layer of lubricant in a manner that the surfaces do not touch each other. Ideally, the hydrodynamic film thickness is several fold greater than the composite surface roughness so that it fully covers the surface asperities and fully protects the mating surfaces. This would imply that the bearing life would be infinite were it not for stop/start or the possibility of contaminants that are always present in the lubricant. Both start/stop and contaminants cause wear and reduce life. Nevertheless, when a fluid-film is present the mode of lubrication is said to be hydrodynamic.

### 2.2.1. Incline-pad and pivoted thrust bearing design.

In conventional thrust bearings, the rotating member—i.e., the slider—is a single, un-segmented surface that slides against a series of stationary pads arranged circumferentially. The stationary pads are separated from each other by deep grooves or channels filled with a lubricant. In the case of the so-called inclined-pad thrust bearing design, the combination of each sliding and stationary body form a convergent wedge, which upon rotation of the slider draws the lubricant inward, completely separates the surfaces and creates hydrodynamic pressure within the bearing clearance. Thus, each pad is capable of generating hydrodynamic load-carrying capacity, and the total load-carrying capacity is simply the summation of the load-carrying capacity of the individual pads. In this type of a bearing, the inclination angle becomes an important design consideration since it is the main agent for creation of the physical wedge, a factor that mathematically represents the “source-term” in the Reynolds equation (Figure 2-10).

An alternative design to the inclined-pad shape configuration is to incorporate a pivot under the stationary pad to allow it to automatically adjust its inclination angle to match the load. The optimum pivot location is typically about 60% away from the inlet. If the pivot is placed at the optimum location, the sliding direction must be such that maximum and minimum film thicknesses are, respectively, at the inlet and outlet, so that physical wedge forms from the high film thickness to low film thickness. This implies that the bearing cannot operate in bi-directional mode. If the pivot is placed centrally at 50% location, then the bearing operates analogously to that of a zero-inclination angle thrust bearing. That is, theoretically the stationary and the slider surfaces are parallel, and surfaces cannot hydrodynamically generate load-carrying capacity. That is to say, mathematically the source term in the Reynolds equation vanishes.

The bearings tested in this study had no pivot point and were simple parallel surface bearings. In practice even parallel surfaces in sliding motion do create some load-carrying capacity due to a variety of factors such as viscosity wedge, density wedge, surface waviness and elastic deformation. Regardless of the underlying physical mechanisms involved, many centrally-loaded bearings function properly, albeit at a lower design load-carrying capacity. Centrally-loaded, pivoted-pad thrust bearings and parallel surface bearings have the advantage of operating in a bi-directional mode. That is, the rotation can be either clock-wise or counter clockwise. Yet surprisingly there is very little information available to assist the engineer at the design stage. The operation of flat, parallel bearings remains, to a large extent, a paradox (Booser & Khonsari, 2010).

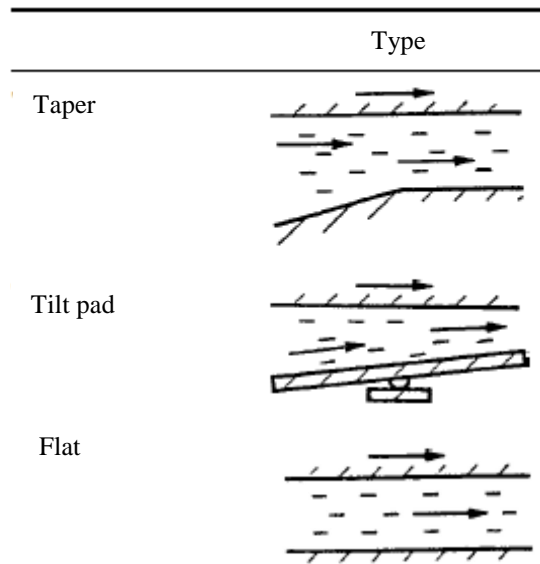


**Figure 2-10.** Schematic of a taper bearing (incline pad with a parallel extension), tilting pad, and flat parallel surface (Source: Khonsari & Booser, 2008).

Referring to Figure 2-11, according to Khonsari and Booser (2008), practically a parallel-surface bearings, or centrally-pivoted thrust bearing, operates at the inlet-to-outlet film ratio of  $a = \frac{h_1}{h_2} = 2$ . This is a very useful and an important guideline for bearing design.

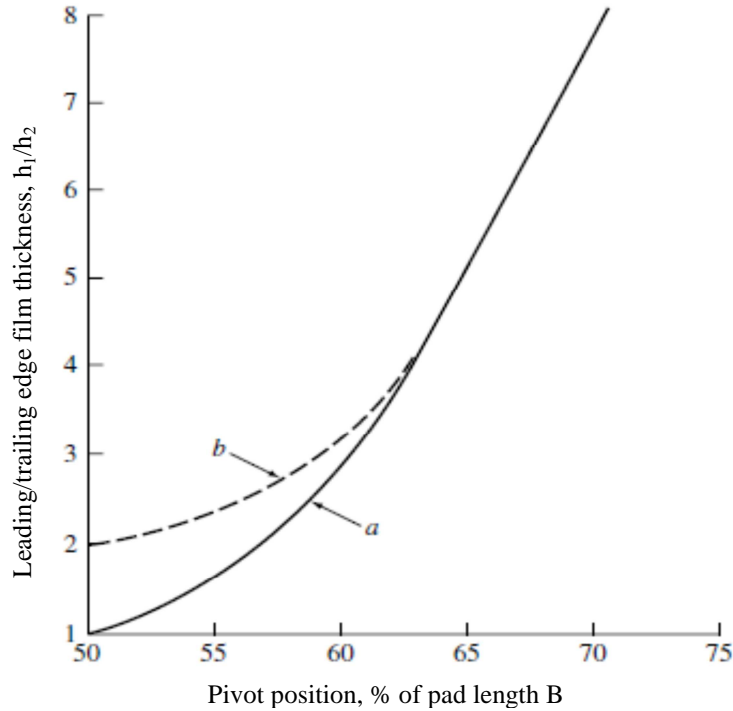


**Figure 2-11.** Film thickness variation with change in the pivot location. Curve (a) is based on rigid flat analysis and the dashed line (b) is based on experience including thermal and pressure-induced deflection in a conventional thrust bearing (Source: Khonsari & Booser, 2008).

### 2.2.2. PCD thrust bearings and highly-loaded bearing operation

The first generation of the USS thrust bearings utilizes a series of circular-shaped pads made of polycrystalline diamond compact (PDC) placed circumferentially on the stationary and rotating parts. To evaluate friction, experimental tests are conducted on a test rig designed and built at USS. This rig is capable of running a wide range of speeds (0-3000 rpm) and load (0-60000 lbf).

When a bearing operates under extremely high load, the hydrodynamic action may be very small and the surfaces come into an intimate contact. As a result, there is significant heat generated in the bearing, which if excessive can result in bearing failure. To this end, PCD pads are extremely valuable for their superior thermo-mechanical properties. Specifically, the thermal conductivity of diamond is 12-fold greater than that of the stainless steel counterpart and this is the major advantage of PCD bearings. Interestingly, extensive experimental testing data with PCD thrust bearings as performed by USS reveal that these bearings can operate in the hydrodynamic regime. Specifically, the results of the friction coefficient when plotted as a function of the operating speed appear to show similar Stribeck-type behavior normally observed in conventional bearings (Stribeck, 1902). (Figure 2-12)

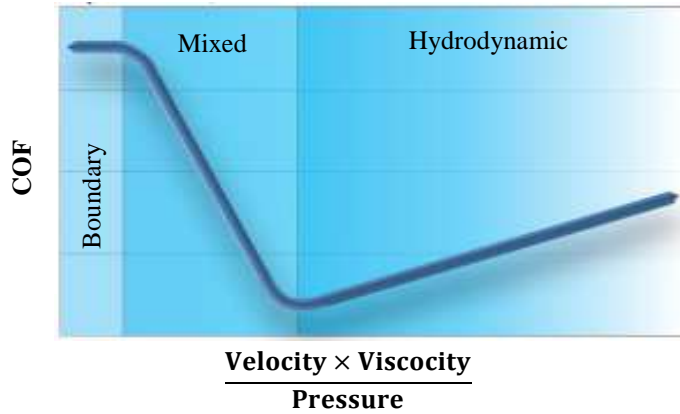


**Figure 2-12.** Stribeck curve relating lubrication regime and friction coefficient to viscosity, rotational velocity, and pressure.

### 2.2.3. Diamond-pad shapes

Diamond bearing pads can take on different shapes and configurations. The original pad shapes pertaining to this project were circular. However, more recently, USS Bearings has developed bearing pads of wedge-shape configuration. In what follows we discuss the pertinent conclusions from testing for both circular and wedge-shape pads. Note that in contrast to conventional bearings, both the slider and the stationary pads are segmented and distributed circumferentially.

### 2.2.4. Design considerations I: Summary

In summary, for conventional and diamond plane or sliding bearings there are several modes or regimes of lubrication. Refer to Figure 2-12:

- During rubbing contact in the presence of a liquid lubricant, there is contact between the high spots, asperities (boundary lubrication). Bearing wear would occur and friction results because of the asperities bumping and shearing as the two surfaces move past each other.
- As speed increases, there is both rubbing contact and the beginning development of a pressurized film (mixed mode lubrication), bearing wear would be reduced but it still occurs.
- As speed increases further, the surfaces are completely separated by a fluid-film and there is no contact of the surfaces. (hydrodynamic lubrication). There would be essentially no diamond wear.

### 3. Bearing development and experimental methodology

Diamond bearings applied to MHK would potentially operate in all lubrication regimes. Therefore, how much the diamond bearing pads wear will be important for determining life estimates and how quickly the bearing develops a fluid-film, also important for efficiency and wear considerations.

All conventional bearing analysis methods assume a continuous runner and most experimental data is based on bearings tested using a continuous runner (Figure 3-1). In contrast diamond bearings must be built from relatively small parts that are formed into tiled or segmented pads. Segmented or pieced together runners had to be developed to accommodate the fact that the size of PCD pad elements is limited by the high pressure sintering constraint. Bearing performance of segmented diamond bearings is, therefore, largely untested, or if testing has been done, it is not published and, therefore, unknown in the industry.

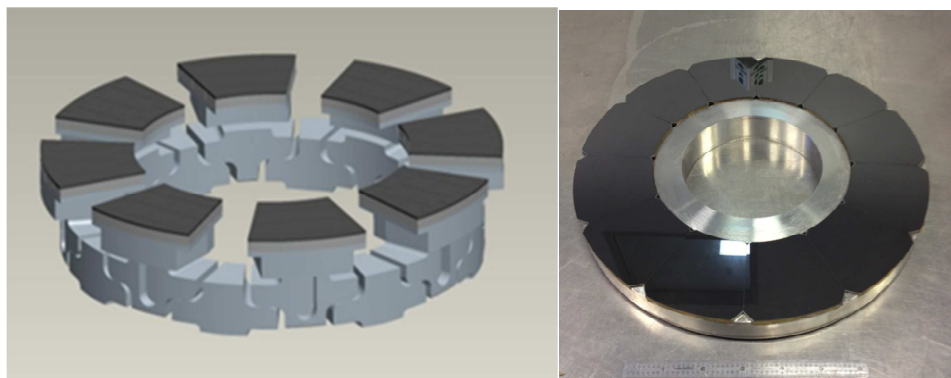


**Figure 3-1.** A tilting pad bearing, model (left), generally has a continuous runner (right).

An experimental and analytical approach had to be developed for this work that would answer the unknowns regarding segmented diamond bearings while also answering whether these bearings would operate well in MHK applications. The developed experimental and analytical approach included:

- Conducting the experiments using water as the lubricating fluid.
- Choosing parameters that reflected the anticipated speeds, loads, cyclical loading, etc. of MHK applications.
- Designing and building three iterations of diamond (segmented) bearings and testing the resulting performance.
- Applying, after each iteration, what was learned to the next iteration;
- Subjecting the final design to cyclical life tests to evaluate the resulting bearing wear. Loads and cycles for life tests were based on a hypothetical tidal turbine operating in a tidal stream with velocities between 0 and 2 mph (MacKay 2009) (Figure 3-2).

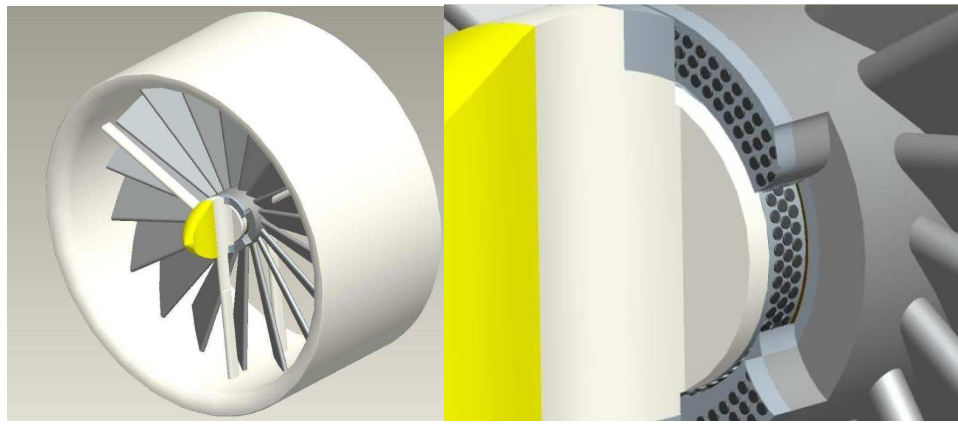


**Figure 3-2.** Hypothetical rendering of an MHK turbine (left), and a cut away view of the turbine revealing a PCD thrust bearing (right).

### 3.1. Analytical model development

It was hoped experimental results could be used to verify new analytical techniques that would account for the segmented nature of the bearing runner and allow us to estimate bearing performance ahead of time. This task proved more difficult than anticipated during the proposal process. Nevertheless, the following was accomplished:

- Design guidelines for circular pads were developed.
- Initial calculations of lift off point or beginning of hydrodynamic behavior were made. (This was found to be very time consuming and not practical for routine design work.)

## 4. Experimental procedure, results and discussion

### 4.1. Experimental procedure

Bearing designs were subjected to the following suite of tests to determine which design would likely perform the best in an actual MHK application and what the advantage of each design might be. Each of three design iterations was subjected to some, but not necessarily all of the following test procedures. Based on the experimental results and the opinions of the study team, the best design was chosen and used as a baseline for the next set of experiments. A total of four experimental sets were conducted with the last set of experiments being life tests where the surviving bearing designs were subjected to cyclical speed and loadings that simulated the conditions of a bearing in an MHK application.

All MHK thrust bearing tests were conducted in the thrust bearing test stand illustrated in Figures 4-1 and 4-2. The thrust bearing assembly is surrounded by a test chamber which serves to retain the bearing cooling and lubricating fluid, a water/glycol mixture. Fluid enters the test chamber at location “A” through the stationary bearing ring and flows around the individual PCD bearing pads on both bearing rings before exiting the chamber at location “B”. In the process of flowing through the chamber, the fluid fills the chamber and completely submerges the bearings. All tests were conducted using distilled water with 5% ethylene glycol to help control corrosion of the test stand. All bearings were run through a “break-in” test at 400 RPM (4.1 ft/s) and 20,000 lbf for approximately 2 hours; this was an attempt to give all bearings the same surface finish to reduce variation in results and improve performance.

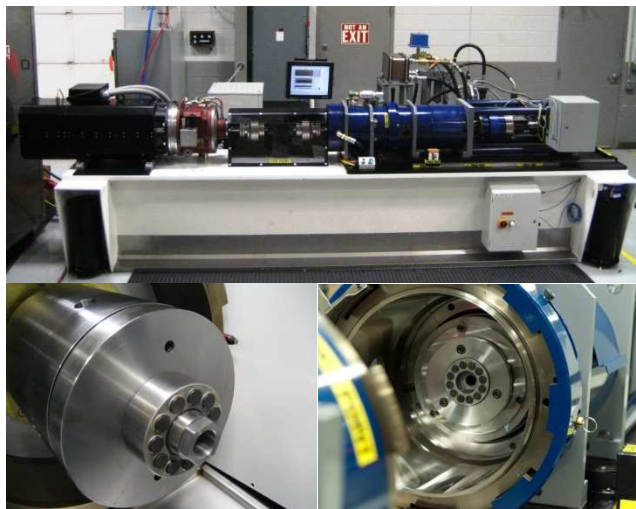


**Fig. 4-1.** Thrust bearing test stand (top) with a rotating thrust bearing (bottom left) and a stationary thrust bearing (bottom right).

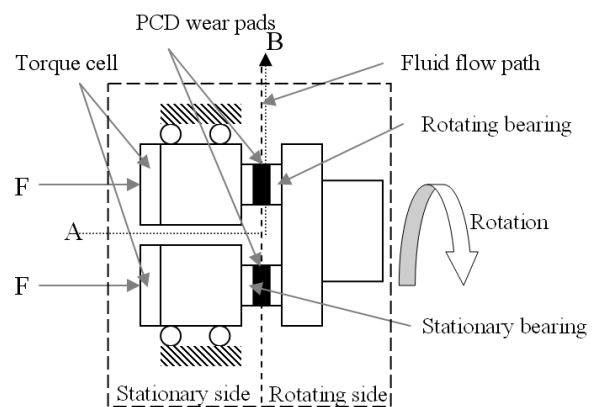


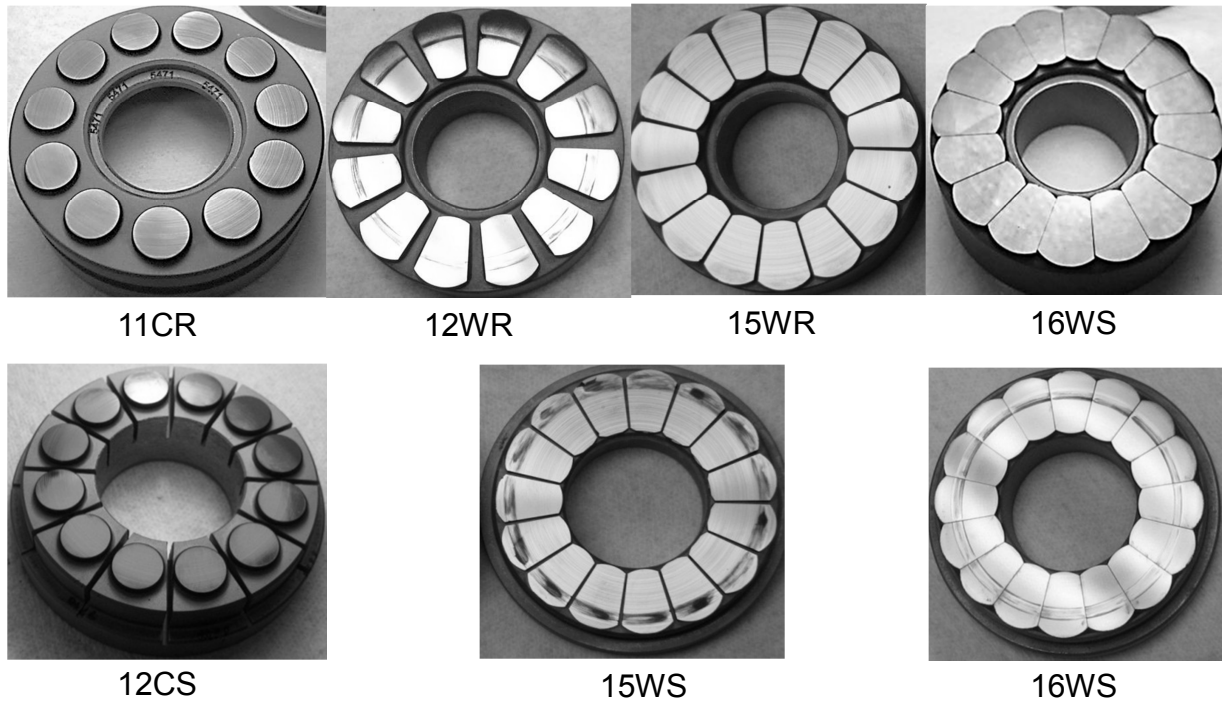
**Fig. 4-2.** Schematic of the thrust bearing test apparatus.

Axial loads were applied to the stationary bearing by a hydraulic ram as indicated by force "F" in Figure 4-2. An electric motor provided the rotation to the rotating bearing. Friction coefficients were determined from torque values measured in a torque cell that was situated directly behind the stationary bearing. Axial load values were also determined using a strain gaged load cell.

As part of the contracted work, modifications were undertaken to the test facility such that the conditions of MHK could be more closely simulated. Specifically, an additional flow loop was added that allowed the circulation of the water/glycol mixture (previously only testing with oil had been done). Control software and hardware were improved to make possible conducting extended tests of several days duration and to perform cyclical tests where both rotational speed and load could be varied to simulate the anticipated MHK environment.

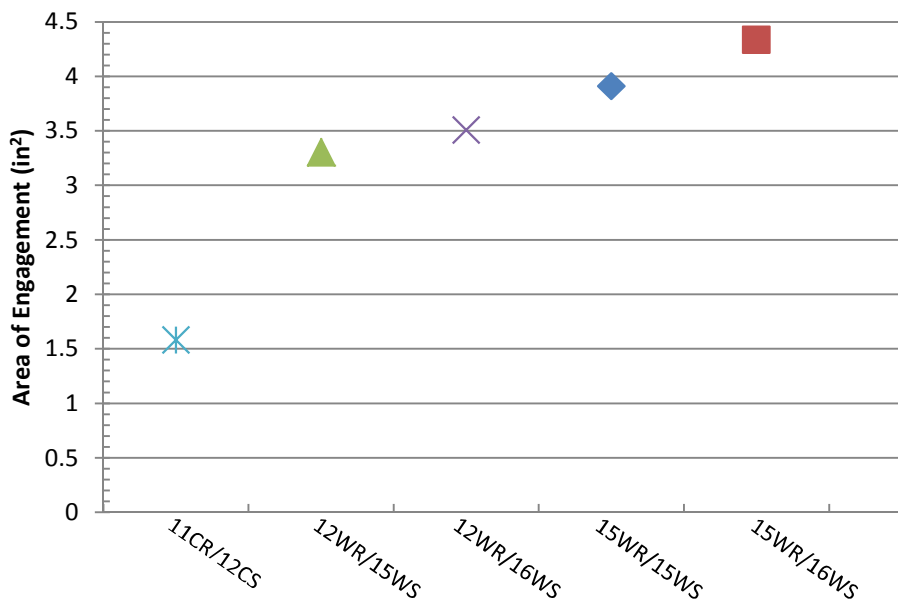
US Synthetic standard test bearing rings are comprised of a circular array of cylindrical PCD wear pads set at a pitch circle of 2.35 inches; the wear pad diameter is .528 inches. The rotating and stationary rings contain 11 and 12 PCD wear pads, respectively. These wear pads are brazed into equally spaced pockets in their respective rotating and stationary stainless steel carrier rings.

Figure 4-3 shows bearing configurations tested through the course of this contract. The configurations discussed were designated as follows: 12WR/15WS, 15WR/16WS, 15WR/15WS, and 11CR/12CS. The number designates the number of pads, the letter (C) or (W) designates circular or wedge-shaped pads, and (R) or (S) denotes whether it is the stationary bearing or the rotating bearing, referred to herein as the rotor and stator. The 11CR/12CS bearings, which are the standard test bearings and described above, were tested for comparison with the hydrodynamic designs, or those bearings using the wedge-shaped pads. These configurations were evaluated in friction, failure, and life (wear) tests as described below. The wedge shaped bearings had the same pitch circle as the standard bearing.



**Fig. 4-3.** Bearing configurations used in the MHK test; the first two numbers indicate the number of inserts on the ring, the first letter designates circular (C) or wedge-shaped pads (W), and the second letter designates a rotor (R) or a stator (S) bearing.

Engaged surface area of each bearing combination is presented in Figure 4-4. This was calculated using solid modeling software and represents the average bearing pad surface area engaged with the mating part. This number stays relatively constant even with relative rotation between the stator and rotor rings with in a tolerance of a few percent. Flow area for each bearing configuration was also calculated and is shown in Figure 4-5. Flow area represents the minimum channel area that the lubricating fluid ‘sees’ as it transits from the inner diameter of the bearing to the outer diameter of bearing during testing. Here, the trend is opposite that of engaged area, e.g. circular bearings had the highest flow area but the least engaged area.



**Fig. 4-4.** Engaged surface area for various bearing configurations.

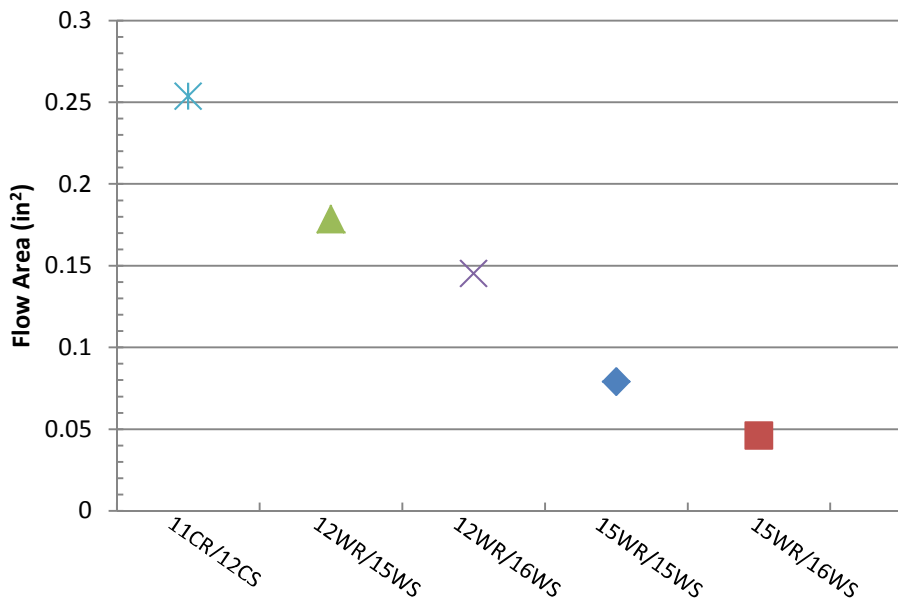


**Fig. 4-5.** Total flow area between pads for various bearing configurations.

## 4.2. Types of tests performed and their purpose

Friction tests were performed with the purpose of determining how quickly the hydrodynamic film was generated and how effectively the bearing configuration carried load. The results from this test are plotted as friction coefficient versus bearing speed. This produces a curve that is much like the classical Stribeck curve as described earlier in Figure 2.12. Each test was performed at constant load and a series of tests were usually performed at several loads from 2000 to 8000 lbf. Comparatively, a bearing whose transition into hydrodynamic lubrication occurs at a lower speed is considered more desirable because of its ability to generate a full-film. This can be determined by examination of the friction test trace creating a distinct minimum. Bearings that demonstrated the lowest friction values at the lowest rotation speeds would be considered best. The least difference in the coefficient of friction traces between high load and low load test cases would mean good load carrying capacity. See Figure 4-8.

Constant load life tests were performed with the purpose of understanding the performance of the bearing over time. Load was held constant at 10000 lbf and speed was held constant at 2000 rpm for 70 hours duration. This is a severe test that always starts out in the mixed mode lubrication regime with the surfaces are in partial contact and, therefore, generating heat and wear. This test quantifies the bearing configuration's ability to withstand premature failure during the 'wear-in' phase of the bearings life. Also, a transition point (TP) or time when the lubrication regime changes from rubbing to hydrodynamic lubrication can be observed. See Figure 4-10.

Bearing load capacity tests were performed to determine at what specific load a bearing configuration fails. During these tests speed was held constant while load was slowly (3 lbf/s) increased until failure occurred. Failure is usually a thermally induced break down of the diamond bearing surface. Cobalt extrusion from within the sintered diamond, surface fracturing, and graphitizing of the diamond are all evidence of thermal failure (Figure 4-6). The bearing that sustains the highest load before failure is considered to have the best load performance. This test is also a measure of a bearing configuration's ability to transfer the generated heat of friction into the cooling lubricant stream. Results are also dependent on how efficient the bearing runs, that is to say, how little heat it produces. This, in turn, is related to how quickly the bearing achieves hydrodynamic running.

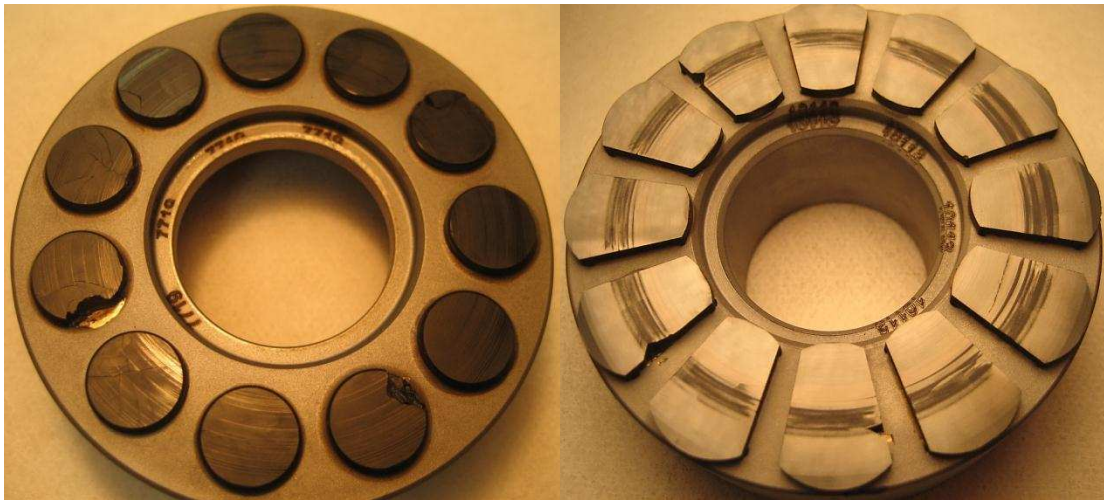


**Fig. 4-6.** Thermal failure in an 11CR bearing (left) and a 12WR bearing (right).

Cyclical loading tests were performed to determine how well a bearing configuration holds up to simulated MHK conditions. Load and speed were cycled to simulate the start and stop of the MHK environment. Load and speed parameters are based on a submerged turbine machine operating in 3 feet/sec flow while subjected to start and stop cycles every 12 hours.

#### 4.3. Results and discussion

##### 4.3.1. First set of experiments

Referring to earlier work using oil as the lubricant, there is a substantial difference in performance between wedge-shaped pads and circular-shaped pads as seen in Figure 4-7. This of course raises this important question; what are the performance differences in water compared to oil? To address this question, the first tests were performed to compare circular versus sector-shaped or wedge-shaped pad performance using water as a lubricant. All testing was performed using a water/glycol mixture for the lubricant. Two wedge-shaped geometries bearing sets, 15WR/16WS and 16WR/15WS, were tried and compared to the circular shaped bearing, 11CR/12CS.

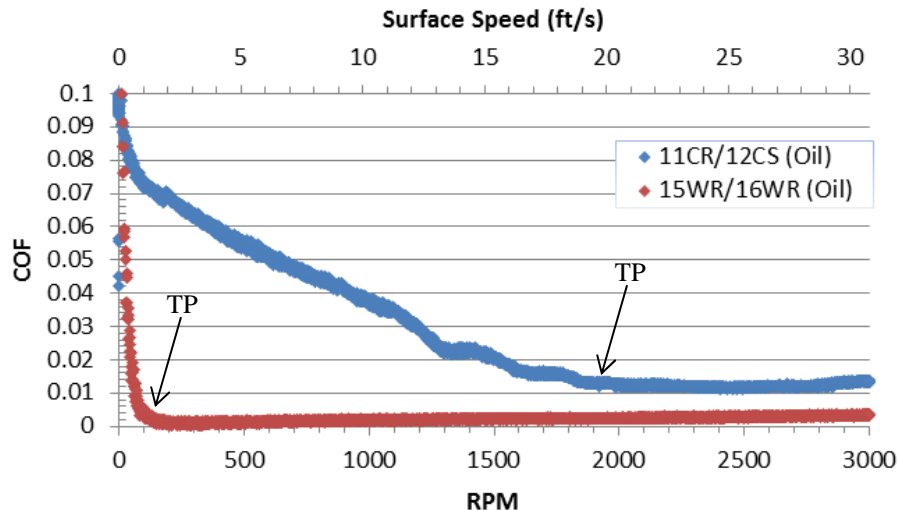


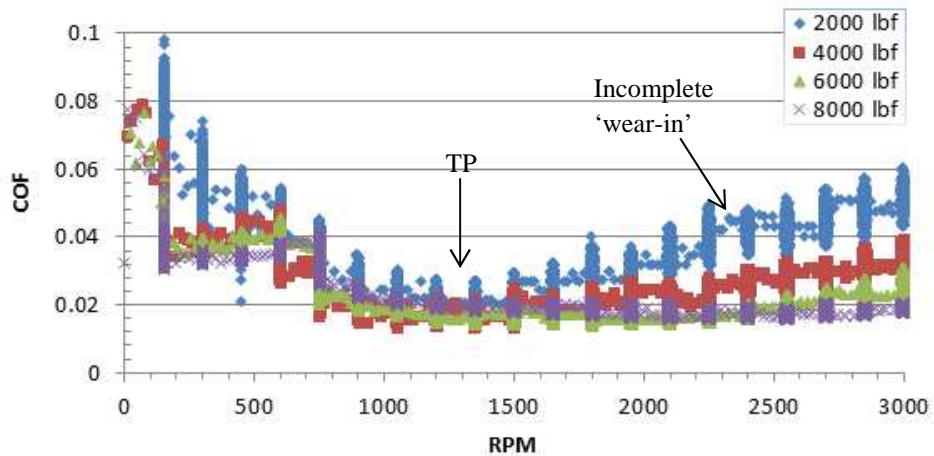
**Fig. 4-7.** COF comparison of circular pads and wedge-shaped pads tested in oil (TP denotes onset of the transition point).

It is important to note that when 16 wedge-shaped diamond bearing pads are used to populate the ring it creates an almost continuous diamond surface. One bearing configuration had this almost continuous diamond surface on the rotor, 16WR/15WS, and the other bearing had the almost same continuous diamond surface on the stator, 15WR/16WS. Both were compared to our standard test bearing, 11CR/12CS, Figure 4-3. The continuous diamond surface on the rotor, 16WR/15WS, possesses the bearing configuration that is most like conventional tilting pad bearings which have rotors that are built with a continuous bearing surface.

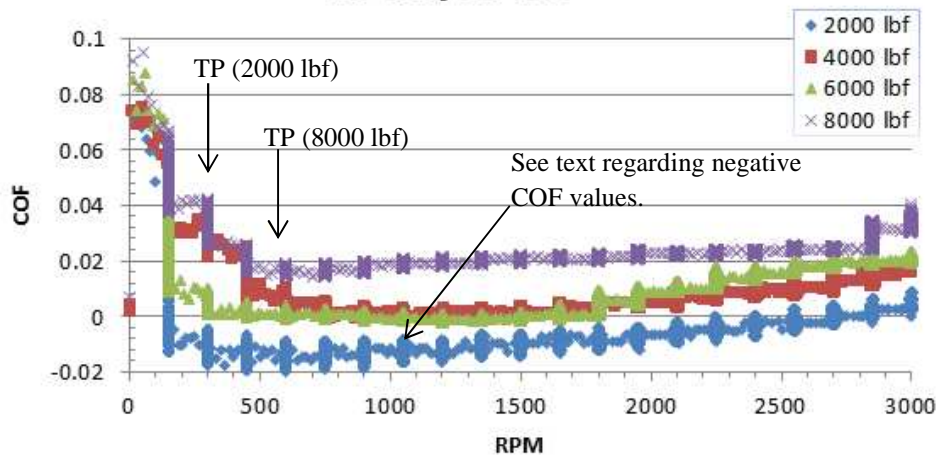
#### 4.3.1.1. Friction tests

Several friction tests were run on each single bearing pair. For each test the load was held constant and the speed, rpm, was increased to 3000 rpm. Tests at loads of 2000, 4000, 6000 and 8000 lbf were conducted for each bearing configuration. RPM was increased in intervals and then held constant for about an hour to allow the torque and bearing temperatures to stabilize. Each test required about 24 hours to complete. COF for each load is plotted versus RPM for each bearing configuration and shown in Figure 4-8.

### 11CR/12CS



### 16WR/15WS



### 15WR/16WS

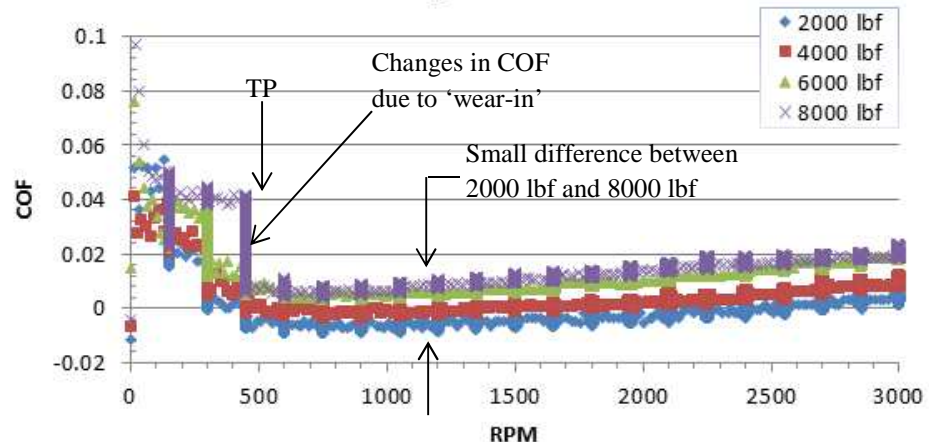


**Fig. 4-8.** COF comparison of 11CR/12CS, 16WR/15WS, and 15WR/16WS configurations versus speed. See text regarding negative COF values.

It was observed that the measured torques were surprising low, in fact, almost below the resolution capability of the load cell. In some cases, negative friction coefficients were recorded which of course are unphysical. This is most likely the result of small calibration errors in the torque load cell that showed up at these low, near the resolution of the torque transducer, readings. This unfortunate uncertainty has made the comparison of the absolute coefficient of friction values of the various bearing configurations problematic. Nevertheless, there are still important differences evident in the data that helped choose the best designs. These will be discussed in due course.

The wedge-shaped bearing with the near continuous pad populated stator, 15WR/16WS performed with the least noise and most consistency. It was most able to carry increased load based on the fact that it had the smallest difference compared to the 2000 lbf and 8000 lbf traces. At lower RPM, levels when the bearings are most probably in mixed-mode lubrication regime, there is considerable variation at each RPM level. The duration of each RPM step is about an hour and it is believed that the change in COF during this time is because of continued ‘wear-in’ of the bearing

The circular pad bearing, 11CR/12CS, showed evidence of partial ‘wear-in’. The 2000 lbf test had a higher friction than the 8000 lbf test. It is assumed that the bearing was still wearing-in during the 2000 lbf test which was performed first and continued to wear-in until the 8000 lbf test which was performed last was complete. Other test results normally show COF increasing as load is increased, see Figure 4-8. In this case, however, it is assumed that the improvement of COF values as load is increased is a result of continued ‘wear-in’ during the entire test.

To confirm the above, detailed COF versus time data are plotted in Figure 4-9 for the 2000 and 8000 lbf traces at 150 and 2850 RPM, respectively. All 2000 lbf traces show significantly higher COF and noisier data than the corresponding 8000 lbf trace. The 8000 lbf trace at 150 RPM shows the remnants of ‘wear-in’ since at the very beginning COF starts out high, but quickly declines to approximately .03. The 8000 lbf data are very smooth when compared to the 2000 lbf trace at the same RPM. At 2850 RPM the 8000 lbf trace is smooth and the COF of friction is lower than all previous traces. The improved bearing performance at 8000 lbf would be consistent with the bearing finally becoming ‘worn-in’ at this point in the test.

## 11CR/12CS

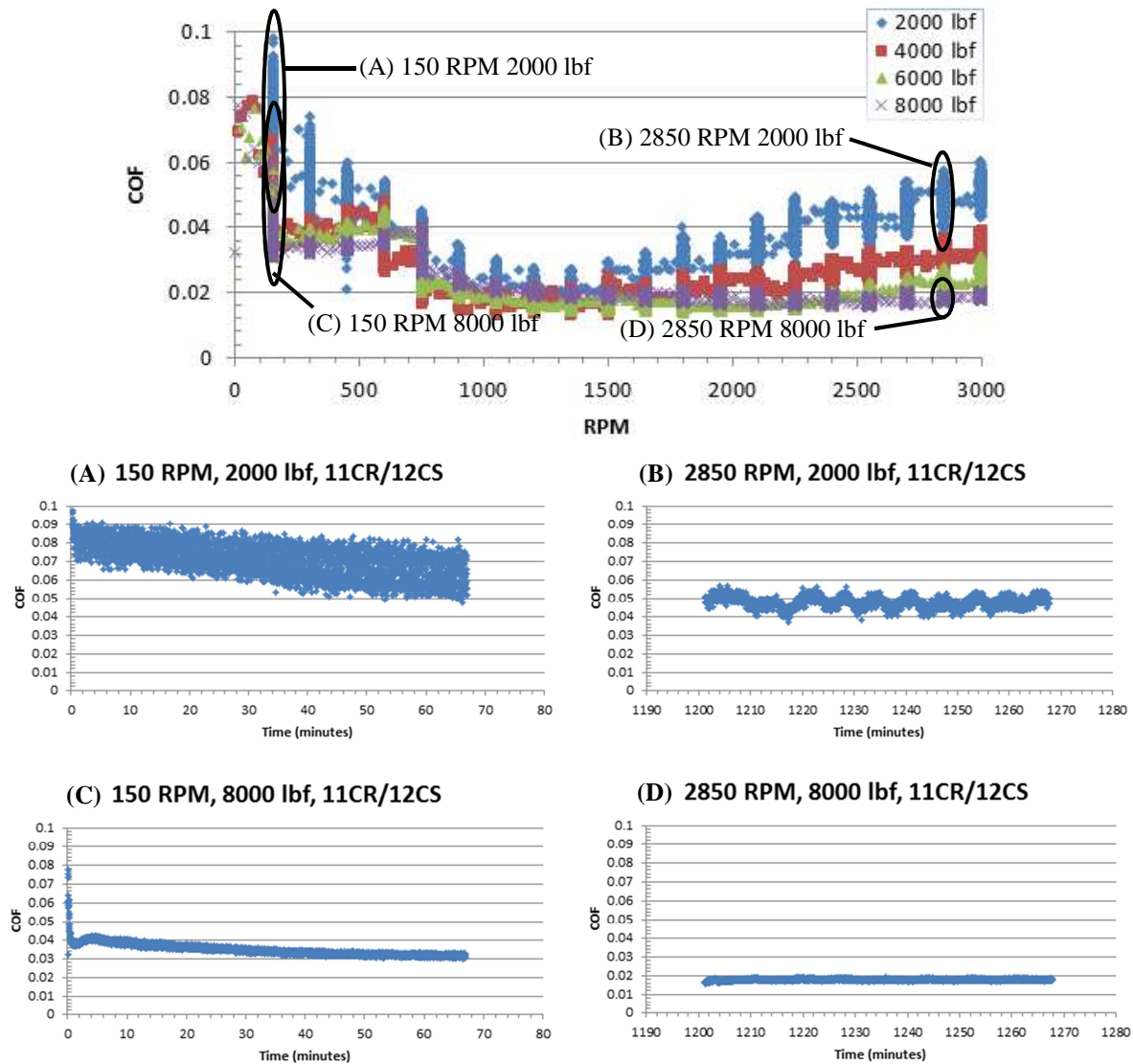
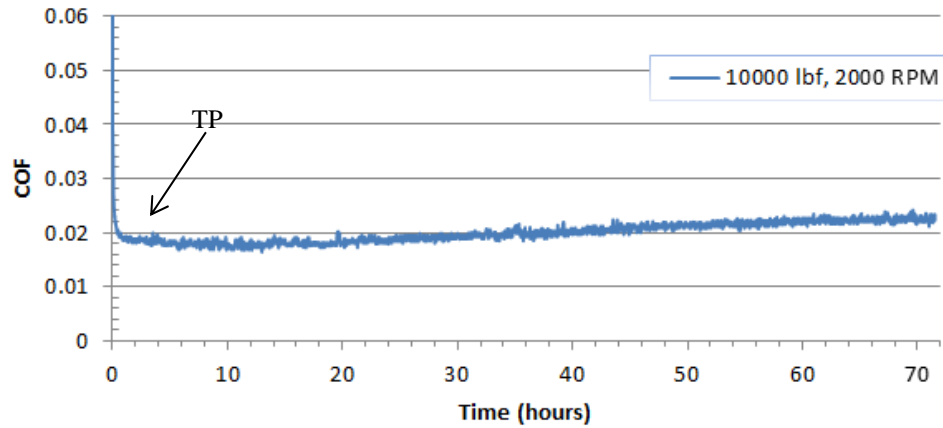


Fig. 4-9. COF versus time for an 11CR/12CS configuration with 2000 and 8000 lbf at 150 and 2850 RPM.

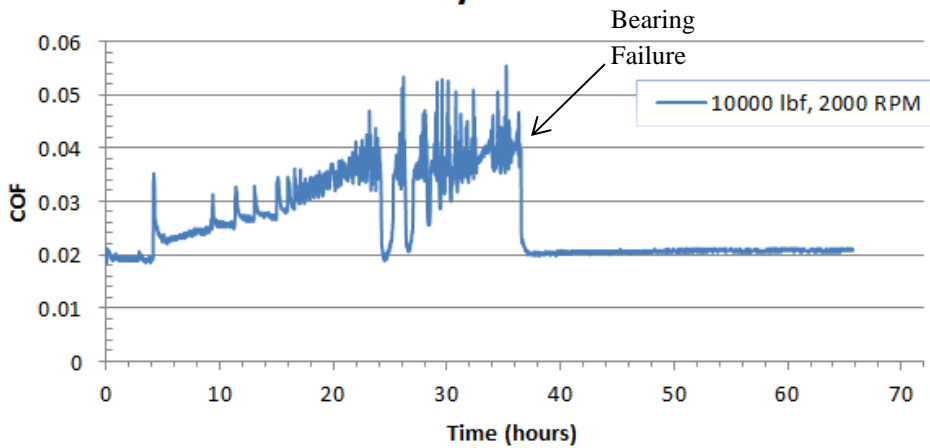
### 4.3.1.2. Constant load life tests

Constant load life tests were performed on these same bearing combinations. These tests were performed, after 'wear-in', at 10,000 lbf and 2000 RPM. The 16WR/15WS failed early at about 35 hours into the test. Note that the rotor had 16 pads which constitute an almost continuous diamond surface. This configuration would be similar to conventional tilting pad bearing architecture as noted earlier. The other two configurations, 15WR/16WS and 11CR/12CS, survived. Both of these bearings had segmented pads on the rotor that are circumferentially distributed. Figure 4-10 presents these data as coefficient of friction plotted against time.

### 11CR/12CS



### 16WR/15WS



### 15WR/16WS

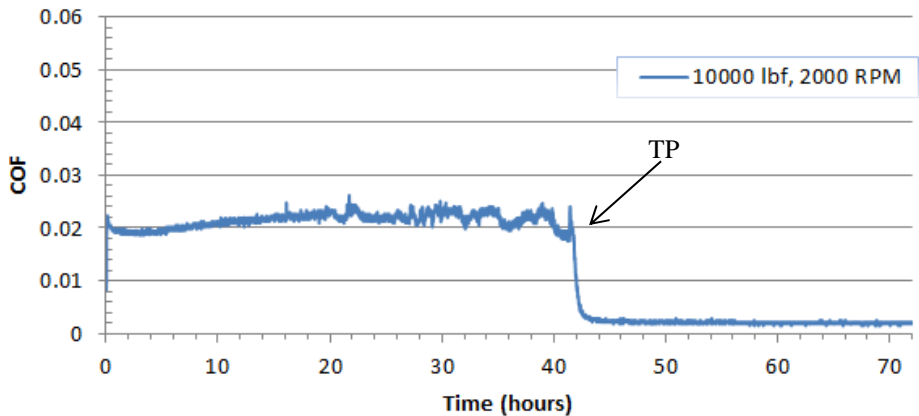


**Fig. 4-10.** COF versus time for 11CR/12CS, 16WR/15WS, and 15WR/16WS configurations during a test with a constant 10,000 lbf load and a constant 2000 RPM speed.

There was a flow rate discrepancy of about one half gallon per minute out of a total of 5 gallons per minute (GPM) flow rate. The 16WR/15WS operated at about 5.0 GPM flow rate. Due to the unexpected pumping action created by the segmented wedges of the rotating 15 pad geometry of the 15WR/16WS it operated at about 5.5 GPM.

Despite the flow rate differences, which could possibly explain the early failure, the study team was concerned that the 16WR/15WS failed while the other two bearings survived. A subsequent test was conducted that confirmed that the rotor with fewer pads creates a pumping action in the lubricant. This pumping action is believed to be beneficial since it encourages local flow velocities which in turn help with the cooling of the diamond. Therefore, it was decided on future designs to make all rotors with widely spaced pads to encourage pumping action.

#### 4.3.1.3. Lessons learned from the first set of experiments

- Rotating the segmented part is best because of the pumping action on the lubricant and better cooling of the diamond pads.
- Wedge-shaped bearings develop a fluid film at lower speeds compared with round bearing pads.
- Round bearing pads and wedge-shaped pads with almost continuous diamond surface stators survived the constant load life test while the continuous diamond surface rotor did not.
- Despite what was thought to be adequate ‘wear-in’ procedures, there was still evidence of inadequate ‘wear-in’ that affected COF results.

#### 4.3.1.4. Design recommendations based on the first set of experiments

- The study team decided that all future designs would configure the stator as the part with the most bearing pads. This creates a bearing that is different from normal practice where the rotor is a continuous surface and the pad bearing is stationary.
- The study team decided to investigate different combinations of bearing pad densities distributed around the circumference of the rotor and stator.

#### 4.3.2. Second and third set of experiments

The next generation bearing designs for iteration two and three had the following configurations: 11CR/12CS, 15WR/15WS, 15WR/16WS, 12WR/16WS, and 12WR/15WS. Please refer to Figure 4-3. All of these configurations have lower pad count on the rotor as decided in the previous testing. Two had only 12 pads on the rotor, a more wide open configuration with ample space available for lubricant flow through the bearing. See Figure 4-3 and the plot of flow area, Figure 4-5.

Each bearing set was subjected first to the friction testing, then the constant load life test and finally the bearing load capacity test where the bearing was eventually loaded to failure. If the bearing survived the first loading to the machine capacity the speed was increased and the bearing was tested again until failure at the new higher speed. This process was repeated until failure occurred.

#### 4.3.2.1. Friction tests

'Wear-in' and test procedure were performed as previously explained. Plots were prepared as before and are presented in Figure 4-11. For comparison test results from 11CR/12CS and 15WR/16WS of the previous test iteration are presented again.

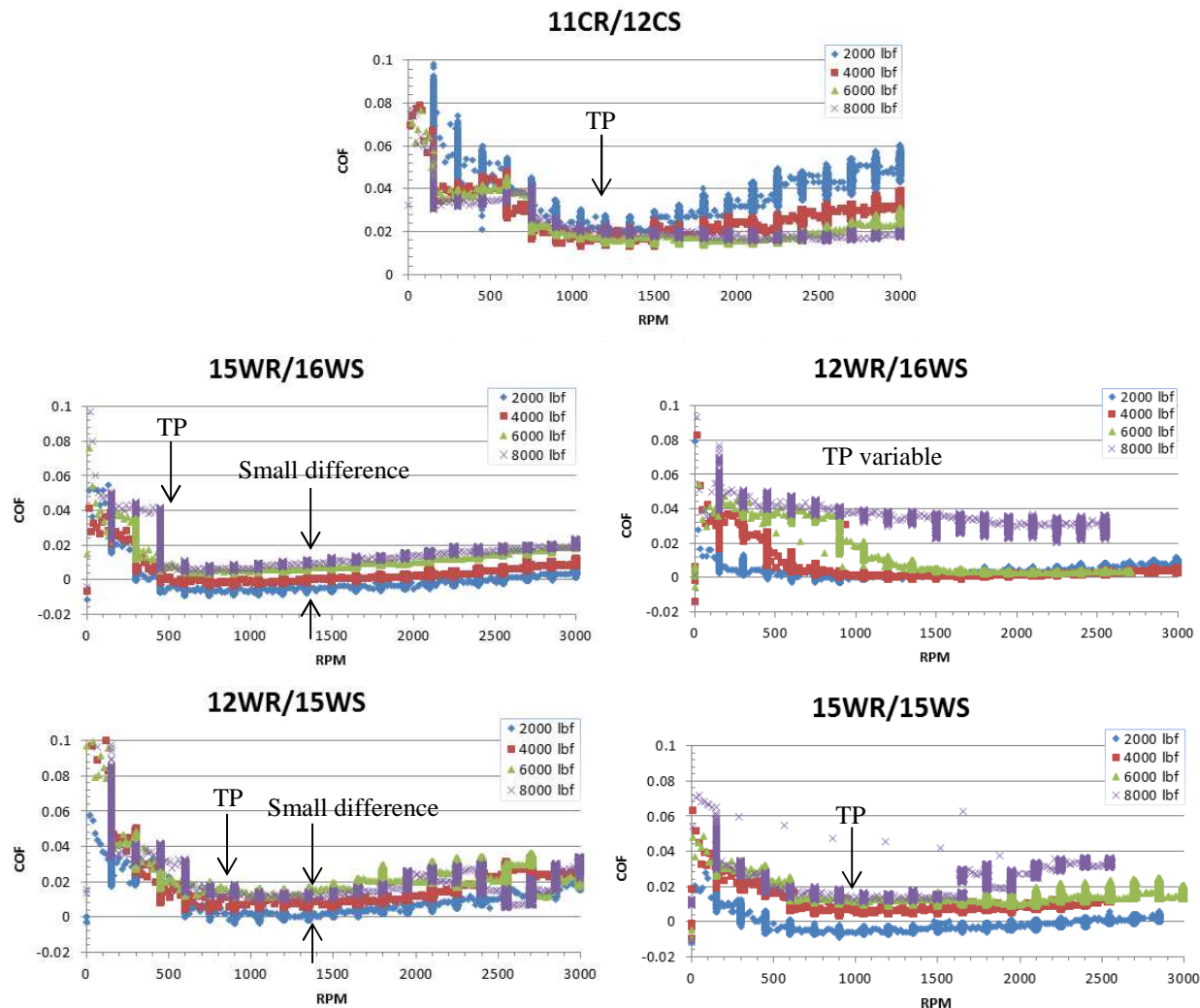


**Fig. 4-11.** COF versus RPM comparison for 11CR/12CS, 16WR/15WS, 15WR/16WS, 12WR/16WS, 12WR/15WS, and 15WR/15WS configurations.

It was observed that all wedge-shaped geometries established fluid-films before the circular counterpart. The 15WR/16WS and the 12WR/16WS tolerated increased loading the best as judged by the relative small differences between the 2000 lbf and 8000 lbf trace. 15WR/15WS ranked second and 12WR/16WS ranked third

Transition points (TP) are labeled on the graphs at the approximate location where hydrodynamic behavior occurred (lift off). This gives an approximate ranking as to which bearing achieves hydrodynamic running the quickest. In this regard 15WR/16WS is the best.

Additional repeat friction tests were performed at 6000 lbf load for the following bearing configurations: 15WR/15WS, 15WR/16WS, 11CR/12CS, and 12WR/15WS and are presented in Figure 4-12. Bearing configurations 15WR/15WS and 12WR/15WS repeated reasonably well with previous tests while bearing configurations 11CR/12CS and 15WR/16WS did not. It is believed the difference between the original and repeat tests results may be because of incomplete ‘wear-in’, similar to what was experienced in the first set of experiments with the 11CR/12CS bearing configuration.

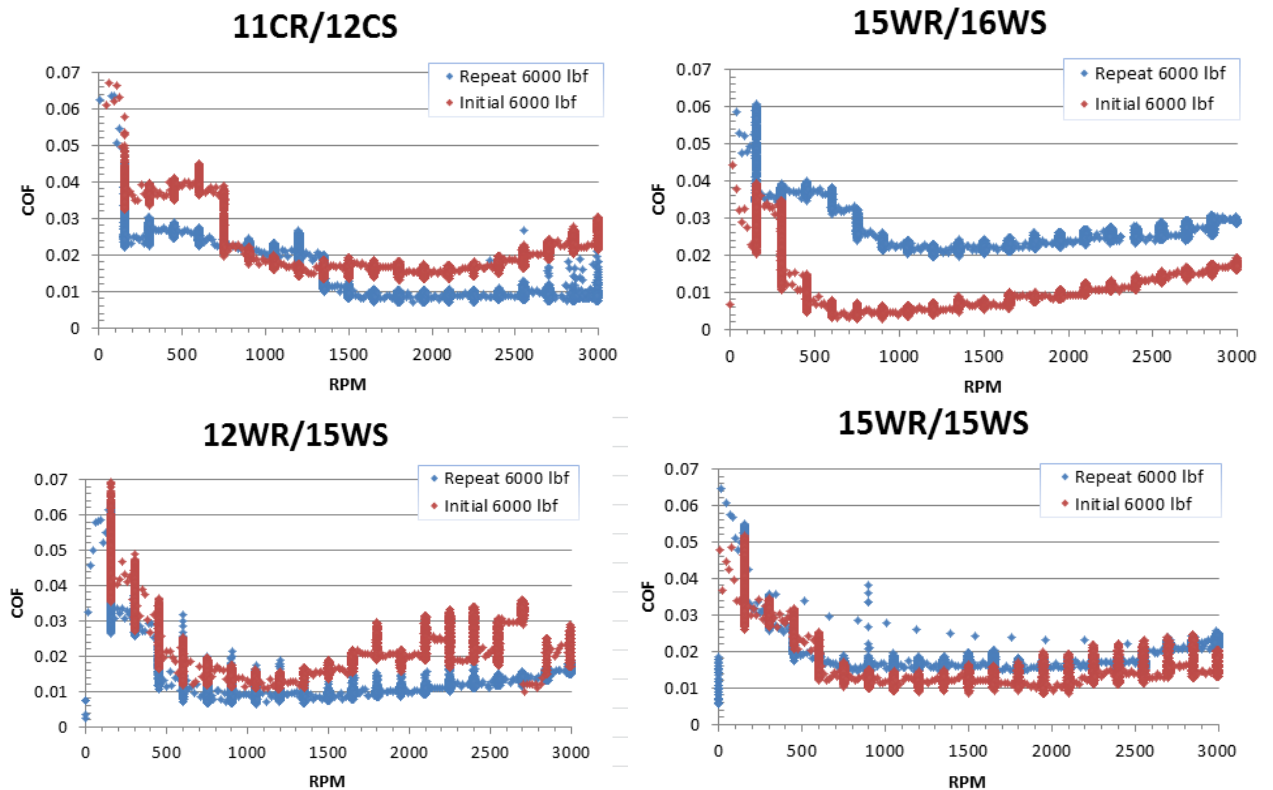


**Fig. 4-12.** COF comparison of 11CR/12CS, 15WR/16WS, 12WR/15WS, and 15WR/15WS configurations versus speed at 6000 lbf repeated friction tests.

#### 4.3.2.2. Constant load life tests

'Wear-in' and test procedures were performed as previously explained. Plots also prepared as before and presented in Figure 4-13. These tests were performed after the friction tests described above on the same set of bearings. For comparison test results from 11CR/12CS and 15WR/16WS of the previous test sequence are presented again. The point at where the bearing 'wore-in' is also indicated with 'TP'.

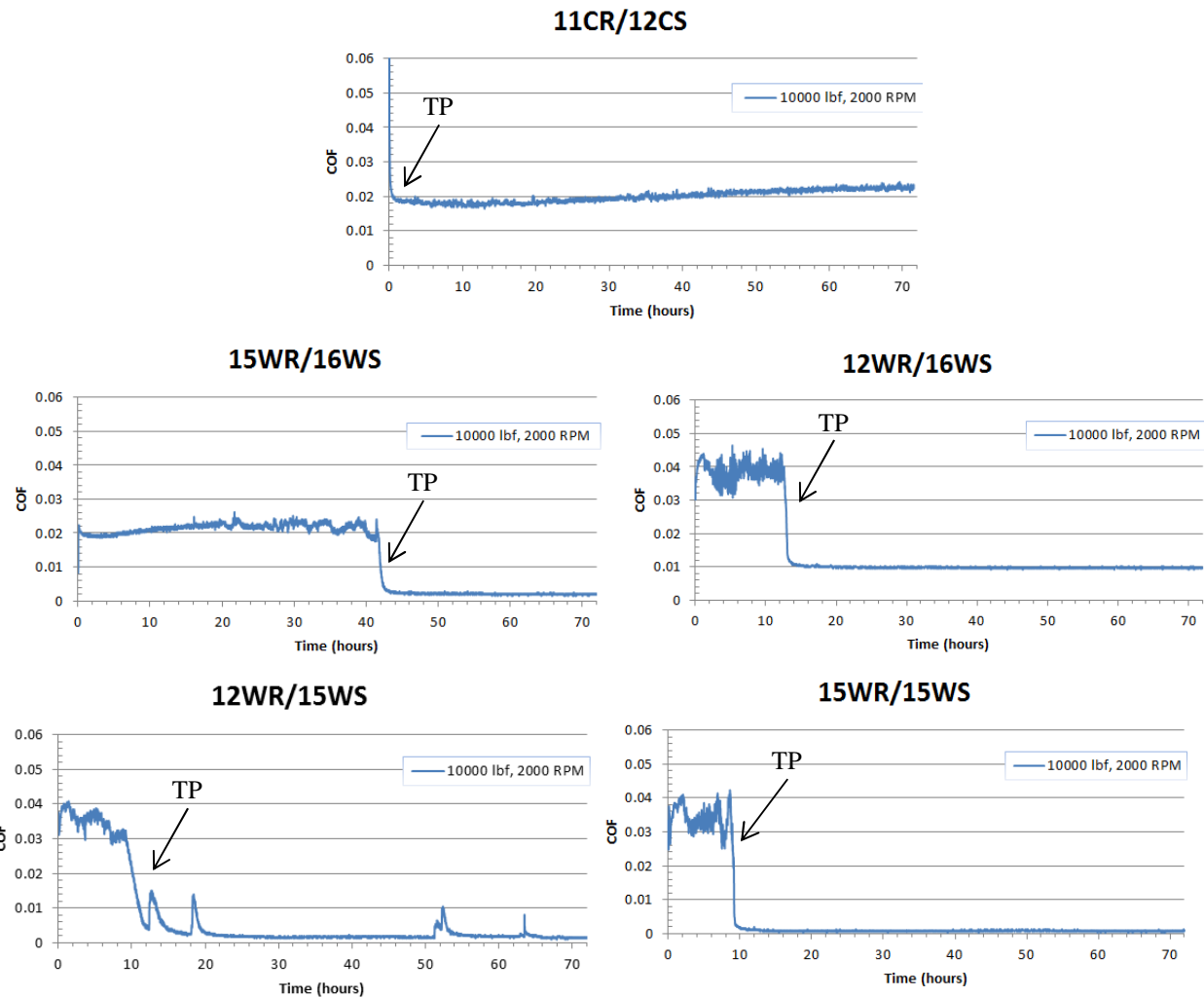


**Fig. 4-13.** COF versus time for 11CR/12CS, 16WR/15WS, 15WR/16WS, 12WR/16WS, 12WR/15WS, and 15WR/15WS configurations during a test with a constant 10,000 lbf load and a constant 2000 RPM speed.

It was observed that all bearings started out at friction coefficients between 0.02 to 0.04. After a ‘wear-in’ time, friction coefficients dramatically reduced to below 0.01 or below. Each bearing ‘wore-in’ at a different time and operated from that point on at low friction levels indicative of a transition to hydrodynamic or fluid-film operation. ‘Wear-in’ times were approximately as follows:

**Table 2.** Approximate ‘wear-in’ time and engagement area of various bearing configurations.

Bearing Configuration	Approximate time to wear-in (hrs)	Engagement area (in <sup>2</sup> )
<b>11CR/12CS</b>	0	1.581
<b>15WR/15WS</b>	9	3.910
<b>12WR/15WS</b>	10	3.306
<b>12WR/16WS</b>	12	3.507
<b>15WR/16WS</b>	42	4.335

Except for 15WR/15WS bearings with more engagement area required longer to ‘wear-in.’

#### 4.3.2.3. Bearing load capacity tests

Bearing load capacity tests were performed at 5 GPM (most of the tests) and later 17 GPM (a few tests). Load at failure and specific load (load/engaged area) are plotted as a function of rotational speed for all the bearing types tested included base line results using oil as the lubricant for comparison, Figures 4-14 and 4-15 (5 GPM). Further, load at failure is shown in separate plots for 400 rpm and 1000 rpm for each bearing type tested, Figures 4-16 and 4-17. An arrow associated with a data point indicates the bearing did not fail and the machine capacity was reached. In such cases, the bearing was re-tested at a higher speed. This procedure was repeated until the bearing eventually failed.

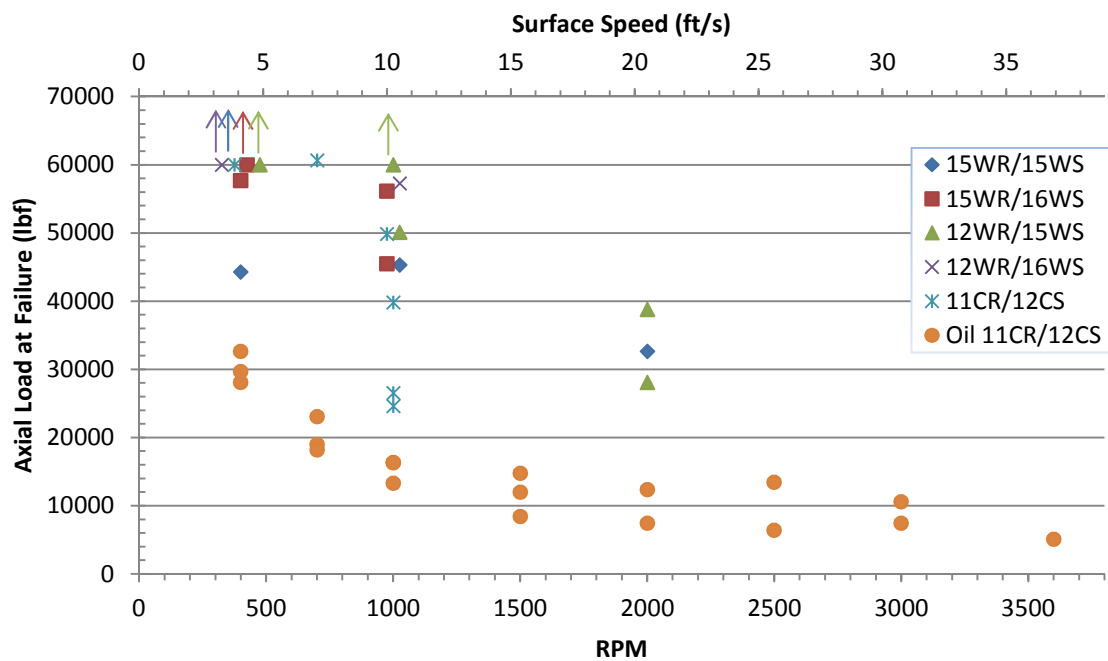


Fig. 4-14. Axial load at failure versus speed for various configurations.

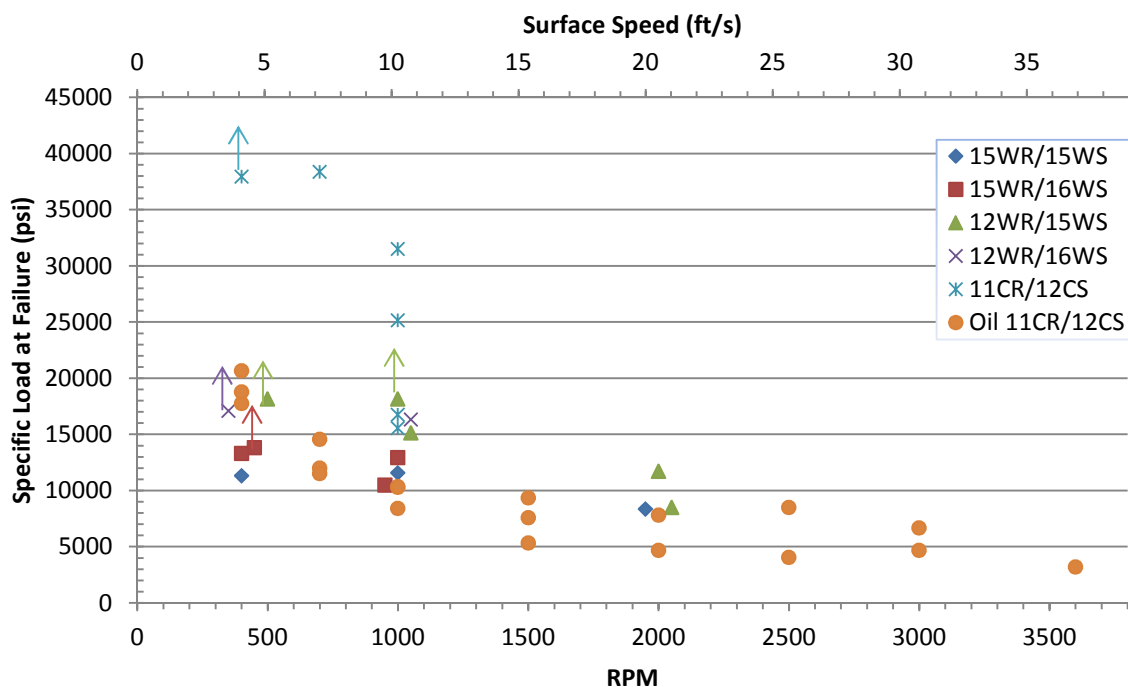


Fig. 4-15. Specific load at failure versus speed for various configurations.

## 400 RPM Failure Tests

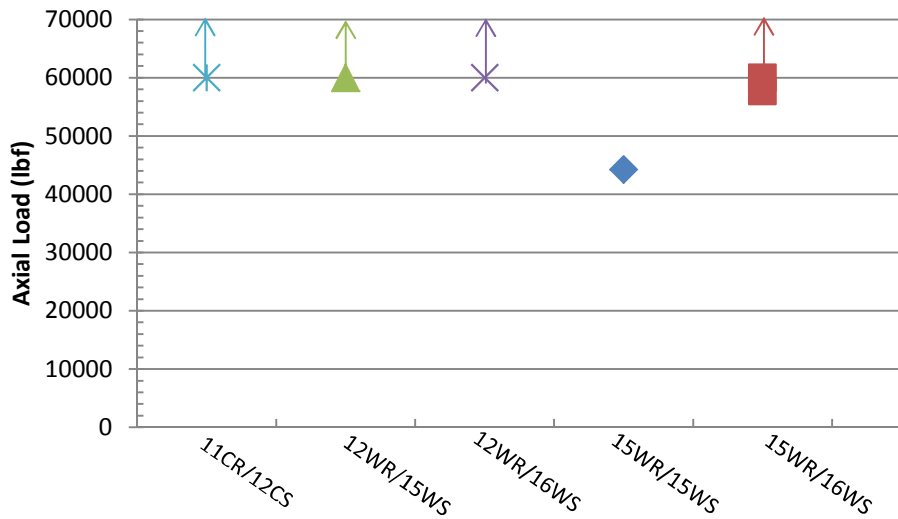


Fig. 4-16. Axial load at failure for various configurations at 400 RPM.

## 1000 RPM Failure Tests

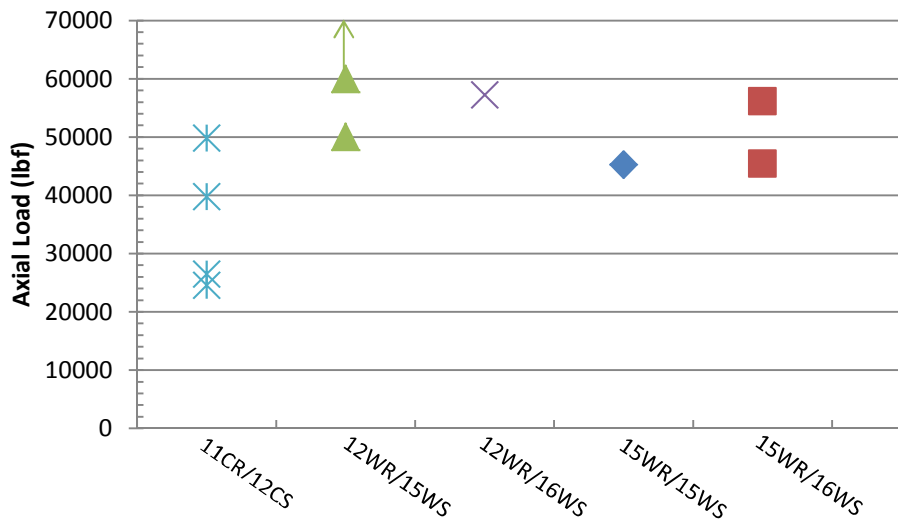


Fig. 4-17. Axial load at failure for various configurations at 1000 RPM.

It was observed that the 12WR/15WS bearing configuration has a high load-carrying capacity (even though the engaged area is not the largest) both with regard to ultimate load and specific load (load/engaged area). The 15WR/15WS configuration was as poor performer except at 2000 RPM. The most data points were available for the round insert bearing, 11CR/12CS. It clearly performed better in water than in oil although there was a lot of variation evident with failure ranging from 22,000 to 50,000 lbf at 1000 RPM. On average, the load at failure was the lowest for the 11CR/12CS bearing of all the bearings tested at 1000 rpm; however, it was a strong performer at 400 RPM. When viewed from specific load (load/engaged area) capacity the 11CR/12CS bearing did better.

At 400 RPM all bearings sustained the load limit of the machine except the 15WR/15WS configuration. It should be noted that at 400 RPM bearing operation for all configurations is not hydrodynamic as seen from the friction testing results presented earlier. This means load carrying ability at 400 RPM in mixed mode lubrication is dictated by how effectively heat can be transferred out of the bearing into the lubricating fluid.

The 11CR/12CS configuration performed well at 400 RPM even though it has significantly less engaged area when compared to the wedged configurations. The reason for this good performance may be the cooling that the open flow geometry of the round parts afford (see the flow area plot, Figure 4-5). In addition, the round bearing pad geometry minimizes the distance from the center and hottest part of the diamond pad to the edge where the cooling fluid takes the heat away.

At 1000 RPM the wedge shaped parts out-performed the circular parts except for bearing configuration 15WR/15WS. Referring to the friction test results at 1000 RPM, wedged-shaped bearing configurations were hydrodynamic or close to being hydrodynamic. The circular parts appeared to be in transition at this speed. This means that the wedged-shaped bearings were operating more efficiently than the circular shaped bearing. This is further substantiated by looking at water temperature differences between the inlet and the outlet of the test apparatus and torque versus thrust load as shown in Figures 4-18 and 4-19.

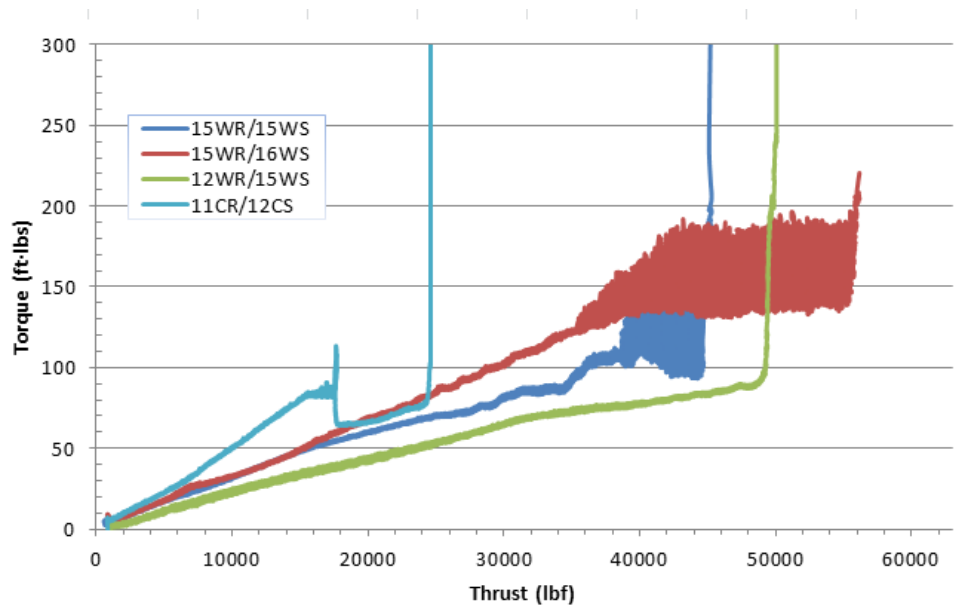


**Fig. 4-18.** Torque versus thrust during a failure test with a constant 5 GPM and 1000 RPM for various configurations.

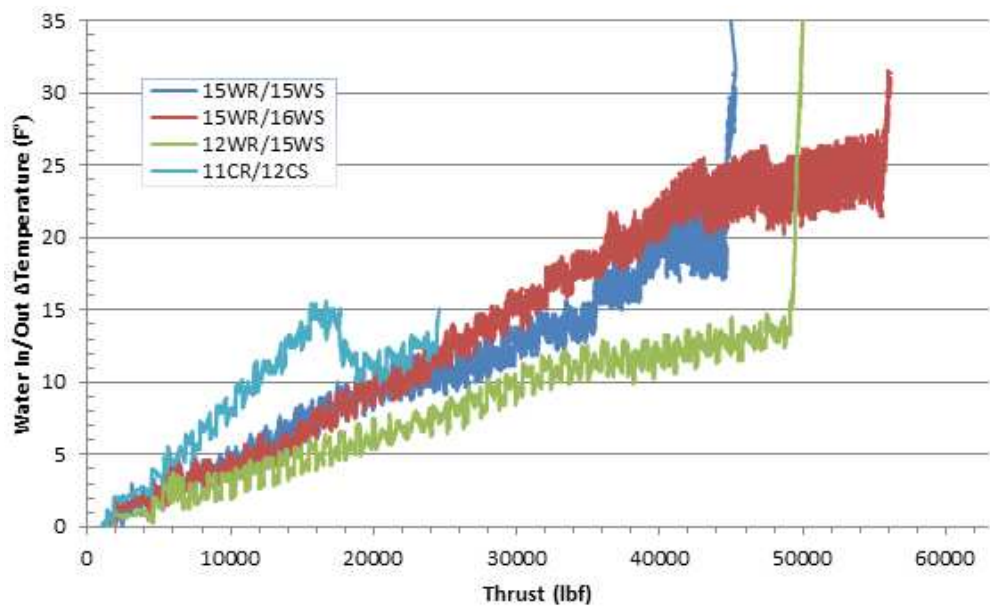


**Fig. 4-19.** Temperature difference versus thrust during a failure test with a constant 5 GPM and 1000 RPM for various configurations.

The 12WR/15WS configuration developed the least torque and temperature difference signaling the most efficient running in combination with the best heat transfer out of the bearing. The 11CR/12CS configuration was the least efficient, but it is known from the 400 RPM capacity tests that it can transfer the frictional heat effectively; so its poor performance is the result of more frictional heating because of the lack of full fluid-film development, i.e. the circular pad bearing was operating in mixed or partial rubbing mode.

Why the 15WR/15WS did not perform well is not known. It has since been learned that failure tests are very sensitive to test apparatus alignment which could be a cause, or it could be that this bearing is not cooled as well as others given its rather constrictive flow area (see Figure 4-5).

In summary the 12WR/15WS and 15WR/16WS showed a slight but not a significant advantage. The 12WR/15WS which has a very open geometry to the cooling fluid performed the best. The good performance is believed to be because this design represents a good compromise between developing a hydrodynamic film at lower speeds and an open design that allows generous access to the diamond for cooling. This is further confirmed by the torque and water temperature difference data which shows the 12WR/15WS operating with the least friction and the lowest temperature difference between inlet and outlet temperatures. Lower temperature difference can mean less contact between surface asperities. This means there less rubbing, more efficient operation, and less bearing surface wear.

Dependence on failure load versus flow rate is presented in Figure 4-20 that plots specific load at failure against flow rate at 1000 RPM. In general, increasing flow rate increases bearing load capacity but not by a large amount and some configurations benefited more than others. The most data are available for the 11CR/12CS configuration where the wide variation in failure load may be due to mixed mode lubrication as can be recalled from looking at the friction test results for 1000 RPM.

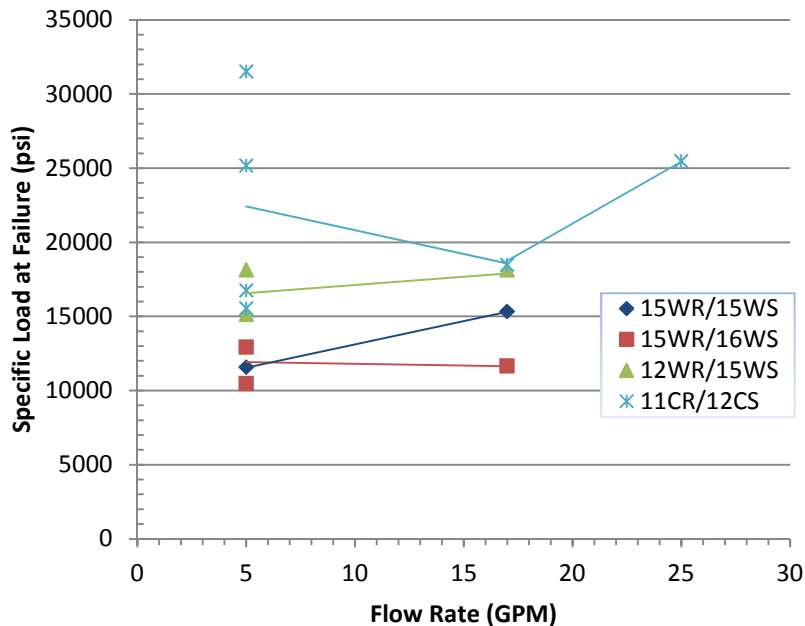


**Fig. 4-20.** Specific load at failure versus flow rate for various configurations.

#### 4.3.2.4. Lessons learned from second and third set of experiments

- From the friction testing the 15WR/16WS best handled increased loading although this capability did not seem to confirm during the repeat test.
- The 15WR/16WS required the longest time to ‘wear in’ as seen from the constant RPM life test.
- Based on the ‘wear-in’ results, bearings with the largest engaged area take the longest to ‘wear-in’.
- From the capacity tests at 400 rpm (in the rubbing mode), all but one of the wedge-shaped bearings reached the limit of machine capacity.
- From the capacity tests at 1000 rpm, the 12WR/15WS operates the most efficiently.

#### 4.3.2.5. Design recommendations based on the second and third set of experiments

- The 12WR/15WS bearing configuration is a good design that combines good hydrodynamic performance with good dissipation of the frictionally generated heat.
- Increasing the flow rate improves load capacity. Nevertheless, the 15WR/16WS performed unexpectedly worse at higher flow rate. It may be that the rather restrictive area available for flow did not allow this bearing to take full advantage of the additional cooling.
- The circular bearing is effective at transferring heat out but does not operate as efficiently at 1000 RPM.

### 4.3.3. Cyclical loading experiments

Life testing was performed using only 2 bearing configurations; 12WR/15WS and 15WR/16WS. These bearing configurations were chosen because they performed well in the friction and failure tests, and because they represented extremes in engaged area for wedge-shaped bearing configurations. These life tests were designed to represent approximately 8 years in the life of a MHK machine. Six thousand cycles were run to represent 6000 tides (diurnal tide) or 3000 days. The rotational speed cycled between 0 RPM and 300 RPM (3.1 ft/s), and the loads cycled from 1500 lbf to 6000 lbf. The speed and load increased from the minimum to the maximum values in one minute. Following a 5 second dwell time the speed and load returned to the minimum values in one minute. Approximately 35 hours were required for 1000 cycles of testing.

All parameters in the life tests were based on the assumptions that typical tidal currents are between 3.3 and 4.9 ft/s and that a tidal stream farm can be evaluated like a wind farm (Mackay, 2009).

#### 4.3.3.1. Life (wear) observations

The tests for both configurations, 12WR/15WS and 15WR/16WS, were carried out without signs of mechanical or thermal failure. Also, both configurations showed improved performance as the test progressed (as the bearings ‘wore-in’). Figure 4-21 shows the cyclic torque during 6000 cycles of the life test for the 12WR/15WS and the 15WR/16WS configurations. In general, the torque decreased overtime. Abrupt reductions in torque were evident in both configurations. These significant changes in torque are a result of bearing ‘wear-in’. When observing the torque data between 1000 and 2000 cycles it appears that 12WR/15WS wore-in faster than 15WR/16WS.

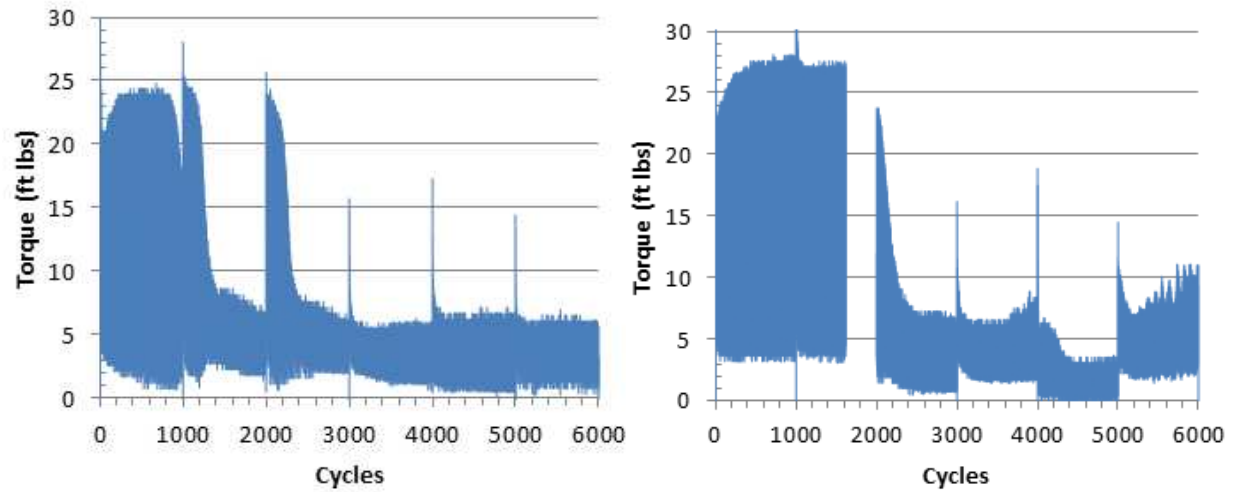


**Fig. 4-21.** Torque over 6000 cycles in the MHK life test for the 12WR/15WS (left) and 15WR/16WS (right) bearing configurations.

The intermittent torque spikes observed in Figure 4-21 at each 1000 cycle mark are due to removal of the bearing from the machine for measurements. At the end of each 1000 cycles, wear and surface roughness were measured. The test bearing required removal from the machine for measurements, and thus, the peaks indicate the beginning of the next 1000 cycle period. The 1000 to 2000 cycle region and the 2000 to 3000 cycle region have a significant reduction in torque. This is probably the result of slight mis-alignment when remounting the bearing.

The surface roughness ( $R_a$ ) of the PCD bearing surface was also recorded. Figure 4-22 shows the decreasing roughness following each 1000 cycle stopping point for the 12WR/15WS configuration. After each period, the bearings were removed from the test machine and the surface roughness was measured. The surface finish improved faster in the tangential direction than the radial direction, since the tangential direction was approximately parallel to the rotational motion. After approximately 3000 cycles, there was little improvement in the surface finish in both the radial and the tangential direction.

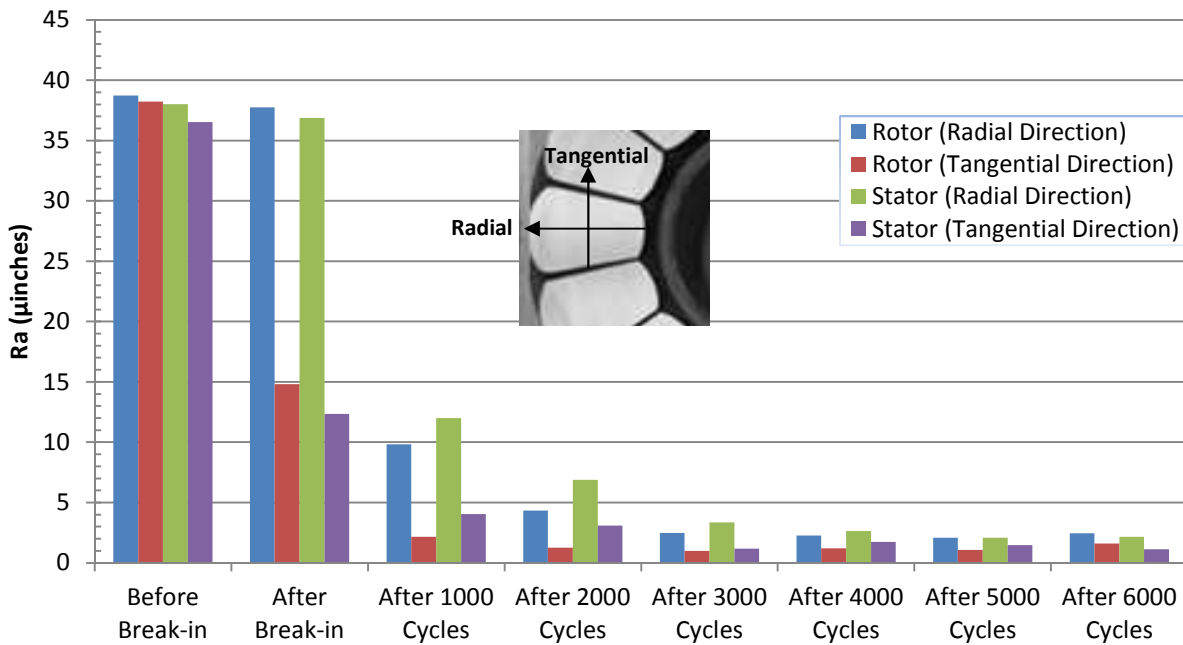


**Fig. 4-22.** Surface roughness over 6000 cycles in the life test for the 12WR/15WS configuration; measurements were taken in the radial direction and the tangential direction.

At each stopping point during the life test, the height of the bearing (i.e. from the bottom of the steel ring to the top of the diamond surface) was measured. The results are found in Figure 4-23. Wear during the ‘wear-in’ period is not included in the Figure 4-22 data.

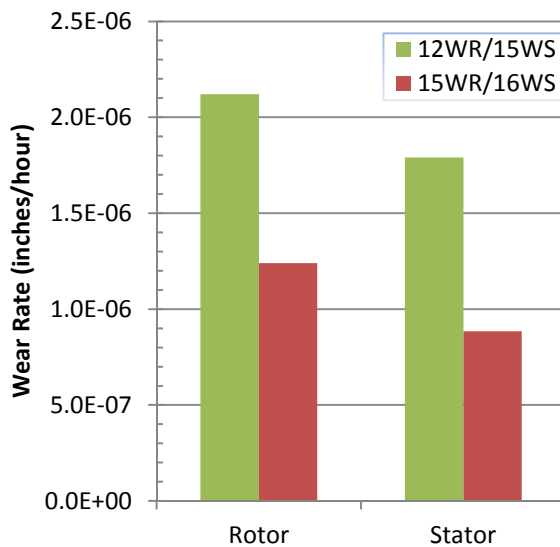


**Fig. 4-23.** Average wear rate during the 6000 cycle life test.

Figure 4-23 shows the 12WR/15WS configuration wore faster than the 15WR/16WS configuration. This could be due to the higher specific loading on the 12WR/15WS. The 12WR/15WS had a maximum specific load of 1800 psi while the specific load on the 15WR/16WS configuration was 1400 psi. Using the highest wear rate from the 12WR/15WS rotor of  $2.1e-6$  inches/hour, it would take over 47,000 working hours (over 5 years) in the thrust bearing test stand under the described parameters to wear 0.1 inches. This is a typical diamond thickness for PCD bearings, but the thickness could be modified to increase the wear life.

A less conservative estimate would be using an  $8.8e-7$  inches/hour wear rate which is based on the average wear rate from the 15WR/16WS stator. This wear rate would result in a total wear of 0.1 inches in 100,000 working hours (approximately 11.5 years).

#### 4.3.3.2. Conclusions from cyclical loading experiments

- Both the 12WR/15WS and the 15WR/16WS bearings survived and performed with minimum wear, while the 15WR/16WS showed the least wear.
- Bearing surface roughness improved dramatically to a polish as the bearings ‘wore-in’.
- Though the wear was minimal it would be advisable for the bearings’ mounts in an MHK apparatus be so designed that minimal wear can be accommodated and still maintain the alignment of critical machine components.

## 5. Design considerations II

### 5.1. Simplified design charts for round-shape pads

The first task of the design study was to determine the feasibility of developing an approximate analytical prediction method for determining the hydrodynamic friction in bearings equipped with round shaped pads in order to establish a basis for future developments.

It is appropriate to point out that all the available thrust bearing design methodologies are limited to sector-shaped pads, not circular. As previously mentioned (Section 2.2.1 referring to Figure 2-11), practical experience indicates that for conventional sector-shaped metal bearings, a film-thickness ratio (inlet to outlet) of  $h_1/h_2 = 2$  can be used for preliminary design calculations (Khonsari and Booser, 2008). While the extent of general applicability of these guidelines for circular-shaped pads made of PCD is not known, it is reasonable to assume that this conclusion applies to round-shape pads as well.

A simplified analysis was developed based on the idea of equivalent areas that converts the results of a “standard square-shaped” pad to that of a circular-shaped pad. The results of the dimensionless load plotted as a function of the film-thickness ratio is presented in Figure 5-1. These results were verified by performing a numerical analysis of the Reynolds equation using the finite difference method. As shown the results labeled “modified square” in dashed lines and circular-shape bearing are in good agreement. Also, shown in this figure are the results of a standard square-shape pad. As shown, the dimensionless load-carrying capacity of a circular-shape pad is lower than that of a square counterpart. This finding, in part, provides a confirmation to the experimental results and conclusions.

Note that as  $h_1/h_2$  approaches unity, i.e. parallel surfaces, the theoretical hydrodynamic load-carrying capacity becomes nil signifying that theoretically the load-carrying capacity diminishes. The associated hydrodynamic friction coefficient corresponding to the same geometries is shown in Figure 5-2.

The use of these figures is only for preliminary predictions and necessarily restricted to hydrodynamic regime. That is to say, after lift-off occurs and surfaces are fully separated. Nevertheless, they are useful for rapid estimation of friction coefficient. If the film thickness ratio were known, one could obtain the load-carrying capacity and operating coefficient of friction. See Appendix 11.3 for a numerical example.

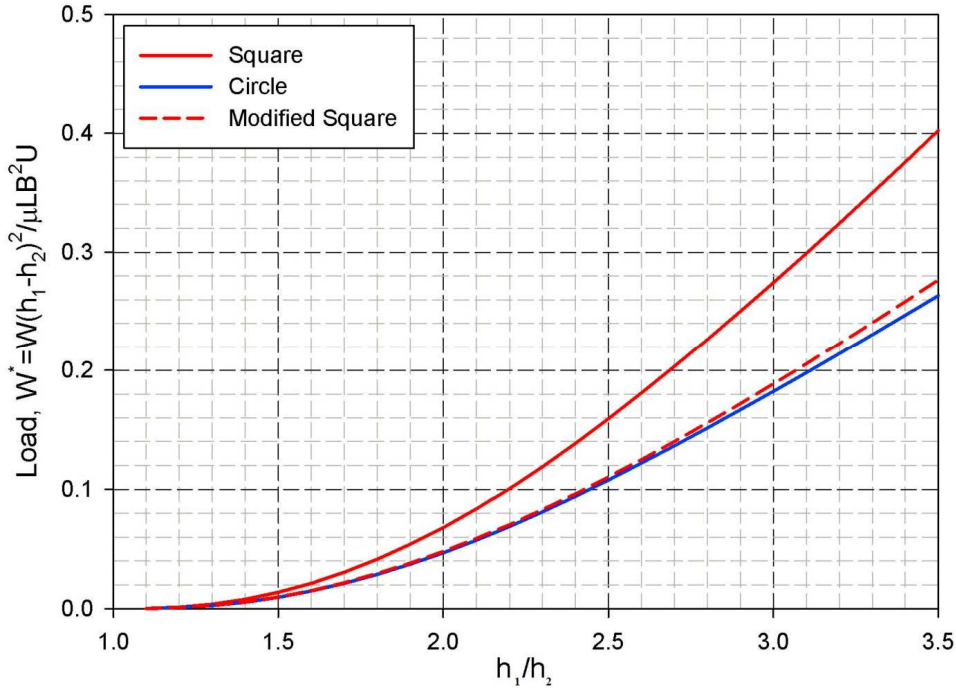


**Fig. 5-1.** Dimensionless hydrodynamic load plotted as a function of film thickness ratio. This figure shows that the results of the approximate solution for modified square and the corresponding circular pad agree well. Here  $W$  represents the applied load,  $L$  and  $B$  are the dimensions of the pad,  $\mu$  denotes the viscosity and  $U$  is the speed of the rotation.

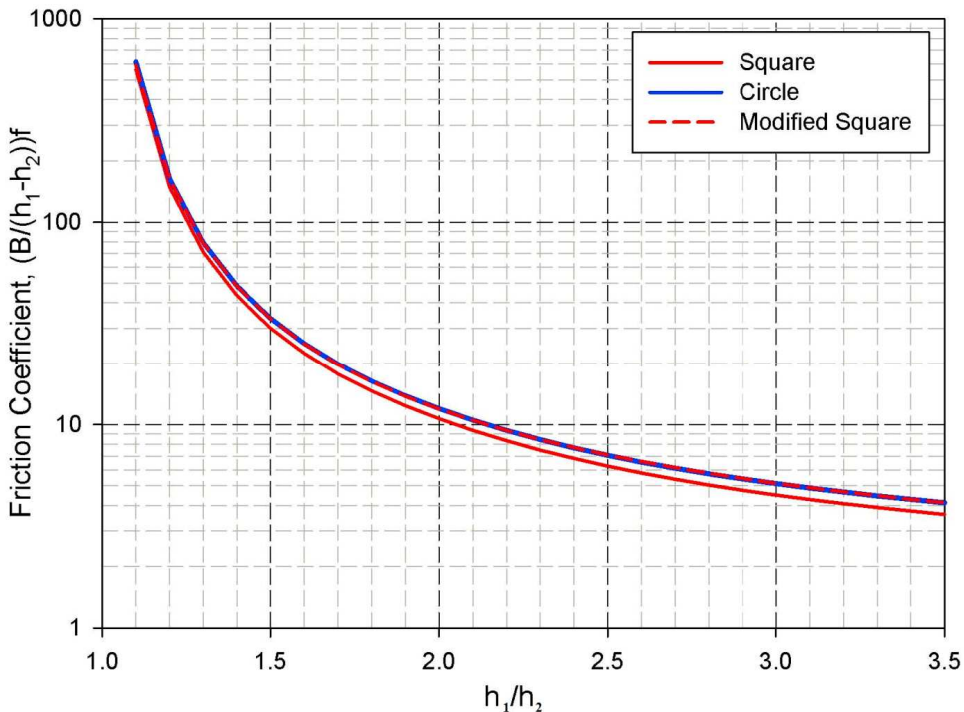


**Fig. 5-2.** Variation of hydrodynamic friction coefficient for a circular pad, its corresponding modified square method and comparison with square. In this figure,  $f$  represents the coefficient of friction.

## 5.2 Lift-off calculations and Stribeck behavior

The determination of the speed at which lift off occurs, i.e. when the bearing operates under hydrodynamic lubrication, is best achieved experimentally. This is typically obtained by examining the behavior of the friction coefficient by fixing the load and increasing the speed. At low speeds, the friction coefficient is relatively large as the bearing operates in the so-called boundary lubrication regime, where the surfaces are in intimate contact. That is, considerable surface asperities of the mating surfaces rub against each and the behavior of the bearing is not governed by fluid mechanics. As the speed increases, the friction coefficient tends to drop, signifying that the fluid (lubricant) begins to contribute to the load-carrying capacity, while still the major portion of the load is supported by the surface asperities. This is often referred to as the mixed lubrication regime. Further increase in the speed typically results in reduction of the friction coefficient as the lubricant begins to contribute to the load-carrying capacity until a minimum value after which friction begins to rise again. The fully hydrodynamic regime is thought to occur after crossing this minimum friction value. This entire friction behavior is often referred to as the Stribeck curve, named after Richard Stribeck (1902). It is often used to differentiate between different regimes of lubrication.

The proper calculation of the behavior of the Stribeck curve in the mixed lubrication regime is quite complex (Khonsari & Booser, 2010) and well beyond the scope of this project. Complexity arises from the interaction between the load-sharing capabilities of the surface asperities together with that of the fluid. This implies that one has to take into account the deformation of the asperities as they are exposed to the external load. The most well-known formula that account for the contribution of asperities is due to work of Greenwood and Williamson's contact model (Greenwood & Williamson, 1966) with the assumption that asperities undergo only elastic deformation. The average load per unit area supported by asperities ( $P_c$ ) can be obtained from

$$P_c = \frac{4}{3} \eta \gamma^{0.5} \sigma^{1.5} E \int_H^\infty (s - H)^{1.5} f(s) ds$$

where  $\gamma$  is the tip radius of asperities (assumed spherical),  $\eta$  represents the asperity density,  $H$  ( $= \frac{h}{\sigma}$ ) denotes the dimensionless surface separation, and  $f(s)$  represents the probability density function., often assumed to be Gaussian for engineering surfaces. The real area of contact is given by

$$A_c = \pi \eta \gamma \sigma E \int_H^\infty (s - H) f(s) ds$$

Using the above equations the total load supported by asperities can be calculated.

Recent application of these equations is given in a paper by Qiu and Khonsari (2011, 2012) in modeling the frictional characteristics of a mechanical seal.

A simplified method was applied to a square-type pad similar to the operation of US Synthetic bearings lubricated with Paratherm fluid with a specified surface roughness to approximately simulate the associated Stribeck behavior. The load was 10,000 lbf supported on 15 pads. The result is shown in Figure 5-3. It is shown that hydrodynamic effect can be expected after about 250 rpm. Similar results are obtained experimentally (see Fig. 4-7). It should be emphasized again, that the detailed analysis of the Stribeck curve and lift off conditions require considerably more detailed analysis, beyond the scope of the work in this project.

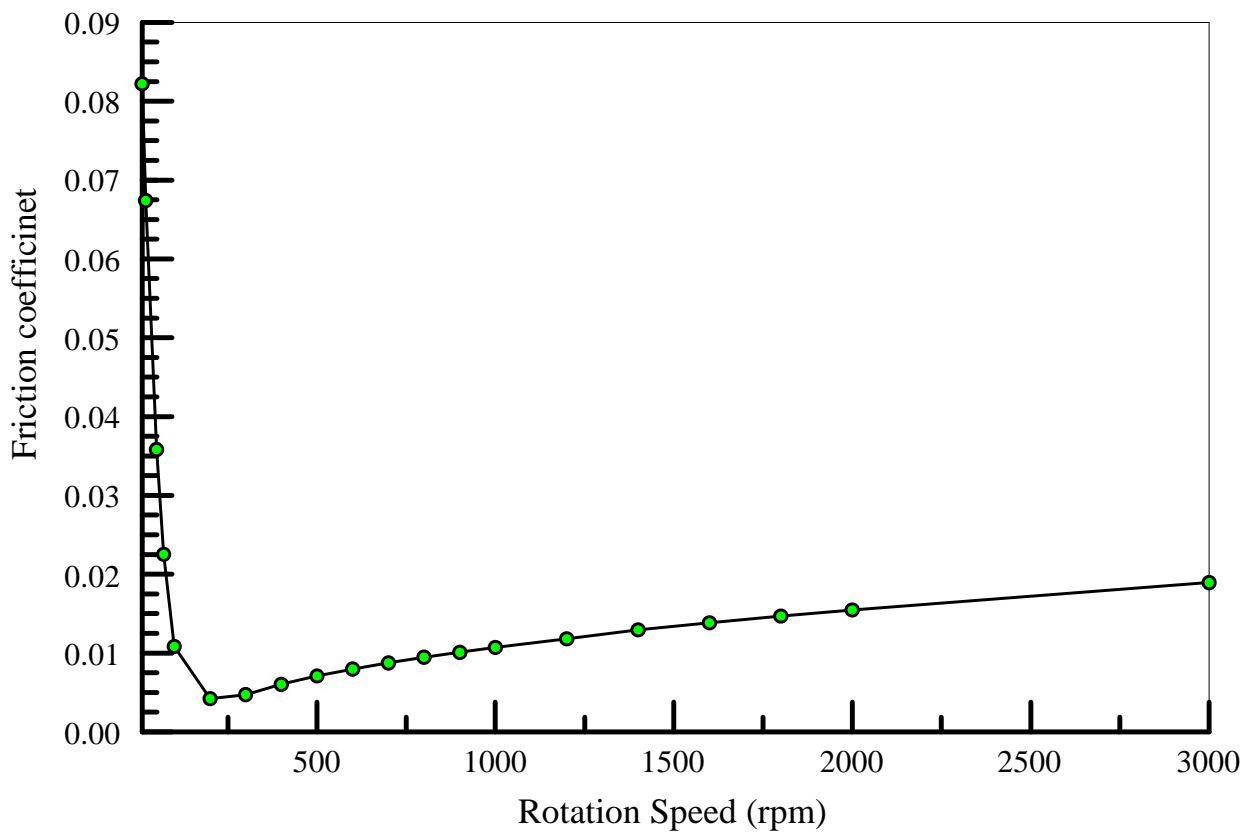


**Fig. 5-3.** Friction behavior as a function of speed.

## 6. Field application of prototype diamond bearings.

The original intent was to provide prototype bearings free of charge for use in actual MHK machines. To that end, several manufacturers of MHK were approached and offered bearings for use in their respective machines. Consistent with the normal adoption of new technology this proved to be a difficult process because of the perceived (or supposed) risk associated with adopting a new technology for such a critical machine component. Thus this research represents a major milestone in providing evidence for the successful utility of diamond bearings in MHK applications.

It is to be mentioned that currently at least one manufacturer is very interested and had USS Bearings develop prototype designs for their apparatus. Upon further consideration, however, this manufacturer decided to wait on the results from an MHK bearing experimental program being conducted at the University of Alaska. USS (as part of this study effort) has already supplied a set of radial test bearings to the University of Alaska evaluation effort.

A solid model rendition of the radial test bearings is shown in Figure 6-1. Field data from their evaluation were not available at the time of the writing of this report.

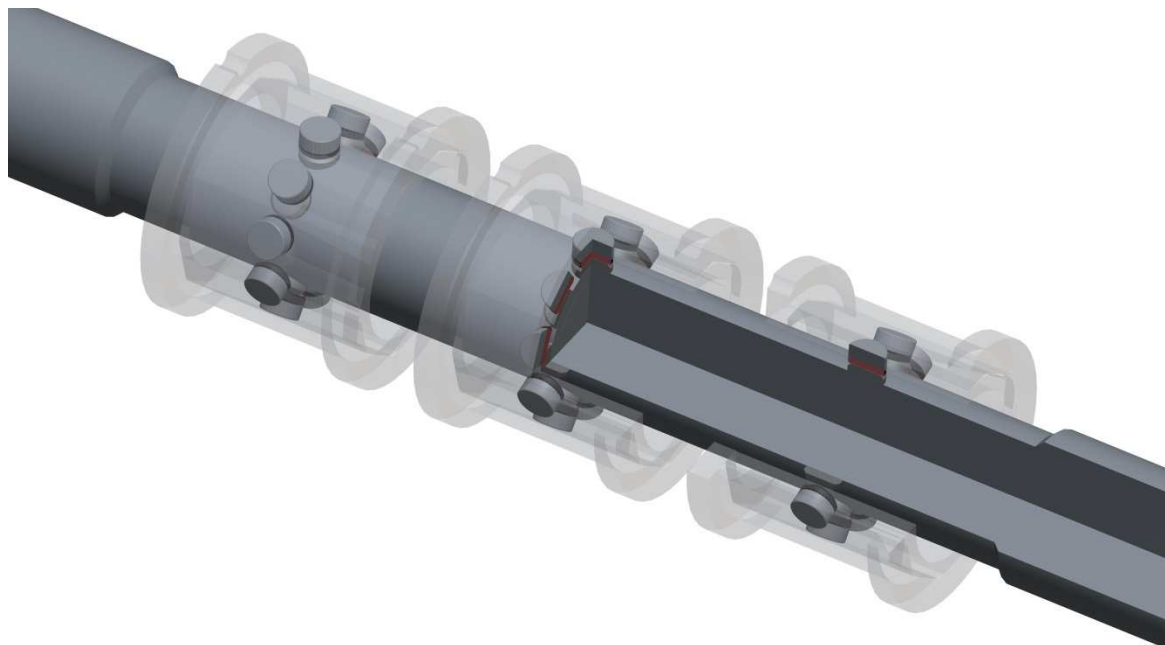


**Fig. 6-1.** Solid 3D model of PCD radial bearings provided to the University of Alaska for testing.

THIS PAGE INTENTIONALLY LEFT BLANK

## 7. Study Summary and Conclusions

- PCD bearings are a good fit for use in MHK machines. They have been shown to:
  - Operate effectively using water as the lubricant.
  - Operate effectively in the mixed-mode lubrication regime that is associated with stopping and starting of an MHK machine operating in tidal flows.
  - Have an estimated life of 11.5 years or more in the MHK environment.
- Diamond bearings for MHK applications are TRL 4 ready; meaning diamond bearing technology is ready to be tested in scaled and full scale MHK machines.
- There is an important trade-off between fluid-film development and heat transfer out of the bearing (for bearings designed to operate in mixed-mode and hydrodynamic lubrication regimes.)
- The rate at which diamond bearings wear and ‘wear-in’ is a function of the engaged diamond surface.
- Reasonable estimates for the performance of round shaped bearing pads can now be made analytically.
- Bearing lift off can be calculated but is very time consuming and complicated and not yet practical for routine design work.

THIS PAGE INTENTIONALLY LEFT BLANK

## 8. Accomplishments

- Developed a viable diamond bearing design for use in MHK.
- Demonstrated the performance of diamond bearings in water.
- Obtained first look at cyclic wear rates with diamond bearings.
- Obtained failure/capacity estimates for diamond bearings operating in water.
- Demonstrated that pad bearings operating in water can develop a fluid-film.
- Showed the exceptional heat transfer properties of water as a lubricant and that this property plays an important role for diamond bearings operating in the rubbing mode in an MHK environment.
- TRL 3 to TRL 4 technical readiness level realized. Diamond bearings ready for testing in prototype and scaled machines.
- US Synthetic participated in the DOE sponsored peer review.
- Placed diamond bearings for experimental evaluation with the University of Alaska, Professor Mohammad Ali.
- Showcased our bearing technology at the 2011 and 2012 ARPA-E symposium.
- Filed one US Patent entitled, “ Bearing Assemblies, Apparatuses, and Motors Assemblies using the Same”, USPTO filing number: 13/550,835.
- Two accepted papers, one presented this year and one will be presented next year:
  - (ASME/STLE) IJTC2012-61061 Polycrystalline Diamond Thrust Bearing Testing and Qualification for Application in Marine Hydrokinetic Machines
  - (WOM) WOM2013-D-12-00285 Polycrystalline diamond bearing testing for marine hydrokinetic application
- Reached out to MHK industry. Currently have three potential customers for diamond bearings.
- Developed the beginning of what could be considered a design methodology for discrete pad bearings as it would pertain to application where both fluid-film and mixed-mode lubrication modes are important.
  - Investigated in detail the performance of round bearing pads and compared those results to rectangular pads. The rectangular geometry is the common geometry for bearing pads.
  - Investigated in detail when hydrodynamic lift would occur. Knowing this would be important for predicting the performance of bearings that will operate both in mixed-mode and hydrodynamic film lubrication regimes.

THIS PAGE INTENTIONALLY LEFT BLANK

## 9. Recommendations

- Though the wear was minimal it would be advisable to design the bearing mounts such that minimal wear can be accommodated and still maintain the alignment of critical machine components.
- US Synthetic should and will continue to reach out to possible users of diamond bearings for MHK and other renewable energy related applications with the intent of commercializing diamond bearings.
- DOE, DARPA, ARPAE and other government entities should become aware of the possible advantages of PCD material. Possible applications include defense related technologies and renewable energy technologies including MHK.

THIS PAGE INTENTIONALLY LEFT BLANK

## 10. References

Booser, E. R. and Khonsari, M. M., 2010, "Flat-Land Thrust Bearing Paradox," *Machine Design*, V. 82, pp. 52-29.

Greenwood, J. A., and Williamson, J. B. P., 1966, "Contact of Nominally Flat Surface," *Proc. R. Soc. London, Ser. A*, 295, pp. 300–319.

Hazen, R. M., 1999, "The Diamond Makers," Cambridge University Press, Cambridge, UK.

MacKay, D. J., 2009, "Sustainable Energy – without the hot air," UIT Cambridge Ltd.

Khonsari, M. M. and Booser, E. R., 2008, "Applied Tribology—Bearing Design and Lubrication," Wiley & Sons, West Sussex, UK.

Khonsari, M. M. and Booser, E. R., 2010, "On the Stribeck Curve," *Recent Developments in Wear Prevention, Friction and Lubrication*, George Nikas, Editor, Old City Publishing, Philadelphia, PA, ISBN 978-81-308-0377-7, pp. 263-278.

Qiu, Y. and Khonsari, M. M., 2011, "Performance Analysis of Full-Film Textured Surfaces with Consideration of Roughness Effects," *ASME Journal of Tribology* V. 133, 021704:1-10.

Qi, Y. and Khonsari, M. M., 2012, "Thermohydrodynamic Analysis of Spiral Groove Mechanical Face Seals for Liquid Applications," *ASME Journal of Tribology*, V., 134, 021703: 1-12.

Stribeck, R., 1902, "Kugellager für beliebige Belastungen," *Zeitschrift des Vereines deutscher Ingenieure*, 46 (37), 1341-1348 (part I), 46 (38), 1432-1438 (part II), 46 (39), 1463-1470.

Surface Technology, 2012, Inc. <http://www.surfacetechnology.com/cdc.html>.

THIS PAGE INTENTIONALLY LEFT BLANK

## 11. Appendices

THIS PAGE INTENTIONALLY LEFT BLANK

## 11.1 Final Technical Progress Report organized by SOPO format

THIS PAGE INTENTIONALLY LEFT BLANK

## Final Technical Progress Report

**Federal Agency to which Report is submitted:** DOE EERE – Wind & Water Power Program

**Recipient:** US Synthetic Corporation, 0893310110000

**Award Number:** DE-EE0003633

**Project Title:** The Development of Open, Water Lubricated Polycrystalline Diamond Thrust Bearings for Use in Marine Hydrokinetic (MHK) Energy Machines

**Project Period:** 09/01/2010 through 08/31/2012

**Principle Investigator:** Craig Cooley, General Manager, [ccoley@ussynthetic.com](mailto:ccoley@ussynthetic.com), 801 319 0891

**Report Submitted by:** Craig Cooley, same as above

**Date of Report:** October 30, 2012

**Covering Period:** Feb, 2011 to Aug 31, 2012

**Report Frequency:** Final

**Working Partners:** Professor Michael Khonsari, Louisiana State University, 1419A Patrick Taylor Hall CEBA, Baton Rouge, LA, [khonsari@me.lsu.edu](mailto:khonsari@me.lsu.edu), mobile: 225-445-6331

**Cost-Sharing Partners:** none

**DOE Project Team:** DOE HQ Program Manager – Jose Zayas

DOE Field Contract Officer – Pamela Brodie

DOE Field Grants Management Specialist – Fania Gordon

DOE Field Project Officer – Nick Johnson

DOE/CNJV Project Monitor

THIS PAGE INTENTIONALLY LEFT BLANK

## ACCOMPLISHMENTS

**Project Objective:** The objective of this project is to demonstrate the feasibility of using polycrystalline diamond (PCD) bearings in marine hydrokinetic energy producing machines.

**Project Goals:** Develop a diamond thrust bearing design that will operate effectively in a MHK machine for an extended period of time without maintenance intervention. To that end the following specific goals have been identified:

- Develop a bearing that performs well in an MHK environment.
- Understand the life expectancy of the bearing developed in '1' above.
- If possible within the project scope, develop a design methodology or design guidelines for MHK diamond bearings.
- Provide proto-type bearings to an MHK manufacturer for field trials.

### **Goal Status:**

#### **Task 1.0 Modify US Synthetic test stand for MHK testing:**

- i. Major activities: As originally planned, successfully modified the US Synthetic flow loop portion of the bearing test apparatus for water flow. In addition modified the test machine control system to permit long duration and cyclical testing.
- ii. Specific objectives: The objective was to make the USS test facility capable of testing thrust bearings under conditions that simulated the actual field application. This required using water as the lubricating fluid and it also required conducted tests over extended periods of times with cyclical loading to imitate tides.
- iii. Significant findings: The modifications were successfully carried out.
- iv. Outcomes: Meaningful testing of thrust bearings for the MHK application was made possible.

#### **Task 2.0 Analytical Design of Thrust Bearings**

- i. Major activities: As originally planned, successfully completed three design iterations for thrust bearings to be used for MHK applications. This task was done in conjunction with Task 3.0. Each time a bearing was designed and then evaluated according to Task 3.0 after which the lessons learned were applied to the next iteration of this task, Task 2.0. This process was repeated three times.
- ii. Specific objectives: The objective of this task was to arrive at a design that would be suitable for use as a bearing be used in an MHK application and suitable for further life testing Task 4.0.
- iii. Significant findings: A significant result of this work was a bearing design that represented a compromise between heat removal from the bearing and good hydrodynamic performance of the bearing. These design constraints compete, thus the resulting bearing was a good first estimate of a compromise between competing bearing architectures.
- iv. Outcomes: The results from Task 2.0 and Task 3.0 substantiated the original thesis that diamond PCD bearings would contribute to the reliability and ultimately the cost effectiveness of MHK.

### **Task 3.0 Bearing Fabrication and Design Confirmation Testing**

- i. Major activities: As originally planned, successfully completed three iterations of friction testing. More than planned, laboratory life testing was conducted to successfully confirm the performance of the bearings. This consisted of unplanned constant load life tests that provided important information regarding bearing durability.
- ii. Specific objectives: The object of this work was to evaluate the designs developed in Task 2.0 of this SOPO with regard to their suitability for use in MHK applications.
- iii. Significant findings: see Task 2.0 above
- iv. Outcomes: see task 2.0 above.

### **Task 4.0 Bearing Life Tests:**

- i. Major activities: As originally planned, four extended life tests were successfully conducted on two bearing designs. Also as planned, multiple tests to failure were conducted on five bearing configurations.
- ii. Specific objectives: The objective was to verify that the bearing designs chosen for the life tests demonstrated sufficient life and durability when subjected to the MHK environment to last at least 5 years and that the configurations were sufficiently durable to withstand anticipated MHK loading conditions.
- iii. Significant findings: A significant result was that both bearing types that were tested easily withstood the life testing and that the majority of the bearings withstood the necessary loading conditions. In addition, PCD bearing wear rates were found to be consistent with an anticipated life of 11.5 years. Finally, it was found that bearing performance improved with time as the bearings ‘wore-in’.
- iv. Outcomes: Results from this task substantiate the thesis that diamond PCD bearings have sufficient life to contribute to the cost effectiveness of MHK.

### **Task 5.0 Modify design methods**

- i. Major activities: A calculation protocol for round pad bearing geometry was developed and calculations were undertaken to determine the lift off velocity (the beginning of fluid-film lubrication) of a rectangular pad bearing.
- ii. Specific objectives: The original objective was to determine a design methodology that would permit the design and calculation of fixed pad diamond bearings for use in MHK based on simulation or mathematical modeling. These objectives were determined to be beyond the realistic scope of the project and were modified to produce a bearing analytical method for predicting the performance of round pads. In addition calculations were performed to analytically determine the speed of the bearing at the beginning of fluid-film lubrication.
- iii. Significant findings: A key finding was that it would be best to determine some bearing performance characteristics experimentally and use the advanced modeling to help in furthering the understanding of bearing performance.
- iv. Outcomes: With the help of experiment and understanding gained from the specific analyses bearings can be developed that will operate effectively in the MHK environment.

### **Task 6.0 Supply of Prototype Test Bearings to MHK Machine Builder**

- i. Major activities: US Synthetic sought out manufacturers of MHK apparatus that could meaningfully evaluate PCD bearings in their respective field trials. Three manufacturers were identified. In the end, one was interested and able to potentially evaluate our bearing. Before using the PCD bearing in the field this manufacturer decided to evaluate the bearing further using the University of Alaska's testing facilities where bearings can be subjected to sand and grit laden lubricating fluids. US Synthetic as part of this contract supplied bearings to the University of Alaska free of charge for this evaluation.
- ii. Specific objectives: The objective is to obtain actual field experience to confirm our laboratory results.
- iii. Significant findings: No field evaluations or test results are yet available although PCD diamond bearings will be evaluated in the next few months.
- iv. Outcomes: Six sets of radial bearings have been fabricated for and provided to free of charge the University of Alaska for evaluation in their test facility. Outcomes from these tests are still pending, however, a key outcome could be the wider acceptance of PCD bearings in MHK devices.

### **Task 7.0 Project management and reporting:**

Project reporting and management was accomplished throughout the project as needed and in a timely manner.

THIS PAGE INTENTIONALLY LEFT BLANK

## 11.2 Discussion of TRL4 justification

THIS PAGE INTENTIONALLY LEFT BLANK

## Technology Readiness Level Advancement from TRL 3 to TRL4

The successful completion of this project as outlined in the SOPO (Appendix 11.2) has advanced PCD diamond bearings from the TRL 3 to TRL4.

In the technology readiness matrix provided with the proposal instructions the funding phase characteristics for TRL3 are described as:

“Design space explored with sufficient analysis to justify detailed design and basic experimental validation. Engineering design is sufficient to justify functional scale model build and backed up by basic small scale model tests.”

The work described in this report has certainly explored the design space experimentally. Confirming tests have been conducted on test bearings under realistic and extreme loading conditions. Evaluation of failure loads, transition from mixed mode to fluid-film lubrication, fixed load life durability and cyclical life durability have all been explored. The MHK environment has been simulated with the use of water as the lubricant. A full environmental simulations using for example salt water laden with potential fouling particles was not undertaken. It is known that from experience using these bearings in drilling fluid lubricated applications in the oil field that grit and sand have no detrimental effect on the bearing and that simulating same would have added substantially to the testing effort with no real added benefit. All testing showed conclusively that these bearings are well suited for application in MHK machines.

As mentioned elsewhere in this report the original intent was to develop an engineering design method specifically suited for segmented PCD bearings. It was soon realized that this was beyond what was possible given the limited time and resources available; nevertheless, limited and useful analyses were conducted to look into the performance of round pad bearings and fluid-film lift off velocities.

It has also been realized through the course of this work that a new method of analysis was not necessary to achieve TRL4 and that traditional analyses for hydro-dynamic and rubbing bearings gives a sufficiently accurate result for a first approximation of the field performance. Despite this US Synthetic is continuing its efforts to develop more accurate models to predict the performance of these bearings using internal funding.

Certainly based on the results of this work it is now possible to design and build a thrust bearing with confidence that would operate successfully in a full scale MHK machine. This fact satisfies the requirements of TRL3 and moves the technology to at least TRL4.

THIS PAGE INTENTIONALLY LEFT BLANK

### 11.3 Example analysis of a round pad bearing

Predict the coefficient of friction and minimum film thickness for a centrally-loaded, pivoted pad circular-shape thrust bearing that can carry a maximum load of 24,279 lbf when rotating at 3000 rpm. The lubricant viscosity is  $\mu = 7.25 \cdot 10^{-7}$  lbf·s/in<sup>2</sup>. The average operating radius (bolt circle) is 4.341 inches. The radius of each pad is 2.461 inches. Assume that 10 pads are to be used.

Since 10 pads are used, the load per pad is:  $W = 2427.9$  lbf

The linear speed is:

$$U = R_{avg} \omega = 4.341 \text{ in} * 3000 \frac{\text{rev}}{\text{min}} * 2\pi \frac{\text{rd}}{\text{rev}} * \frac{1 \text{ min}}{60 \text{ s}} * \frac{1 \text{ ft}}{12 \text{ in}} = 113.6 \text{ ft/s}$$

Assuming that  $h_1/h_2 = 2.0$ , from Figure 5-1, we have  $W^* = 0.05$ .

$$h_1 - h_2 = \left( \frac{LB^2 U \mu W^*}{W} \right)^{0.5}$$

Since  $L=B=2R$ , the above equation simplifies to:

$$h_1 - h_2 = \left( \frac{8R^3 U \mu W^*}{W} \right)^{0.5}$$

Substituting the numerical values in the above equation yields:

$$h_1 - h_2 = \left( \frac{8(2.461)^3(113.6)(12)(7.25 \cdot 10^{-7})(0.05)}{2427.9} \right)^{0.5} = .00156 \text{ inches}$$

Since by assumption,  $h_1 = 2h_2$ , then the minimum film thickness is:

$$h_2 = .000779 \text{ inches} = 779 \mu\text{inches} (19.9 \mu\text{m})$$

Note that this minimum film thickness is obtained assuming that the viscosity remains at the specified value. Therefore, the temperature rise within the bearing must be predicted and the viscosity adjusted in order to obtain a realistic viscosity, which would be expected to be lower than 779  $\mu\text{inches}$ . Several iterations on viscosity may be needed (Khonsari and Booser, 2008). The final value of the minimum film thickness should be checked to ensure that it satisfies the composite surface roughness so that hydrodynamic lubrication can be accommodated. For PCD bearings, this can be easily satisfied.

To determine the COF, we use Figure 5-2. Entering the figure with the same film ratio, we read

$$\frac{B}{h_1 - h_2} f = 14.$$

Solving for COF yields at the above minimum film thickness yields:

$$f = 14 \frac{h_1 - h_2}{R} = 14 \frac{.00156}{2.461} = 9 \times 10^{-3}$$

Having determined the COF, it is easy to determine the friction force and power loss. The result should be multiplied by the number of pads (10 in this case) to determine the total power loss.